REVIEW

Recent progress in the high cycle fatigue behaviour of γ-TiAl alloys

T. E. J. Edwards[a]

[a]Department of Materials Science and Metallurgy, 27 Charles Babbage Rd, University of Cambridge, Cambridge CB3 0FS, UK

ARTICLE HISTORY
Compiled April 4, 2018

ABSTRACT
The high cycle fatigue (HCF) properties of γ-TiAl alloys are reviewed, particularly with regards to the deformation mechanisms active in the near-threshold cyclic loading regime. By examining the influence of lamellar orientation and thickness on the HCF threshold, in addition to more conventional microstructural considerations such as the grain size or the volume fraction of lamellar colonies, factors to improve the γ-TiAl microstructure for HCF are assessed. Finally, experimental methods and loading strategies are surveyed to identify techniques for improving HCF testing of γ-TiAl alloys. In this, we consider both the conservativism of differing approaches, and the possibility to measure with suitable resolution the local mechanical behaviour under HCF of the lamellar γ-TiAl microstructure.

KEYWORDS
Titanium aluminide; high cycle fatigue (HCF); deformation mechanisms; fatigue crack nucleation; fatigue crack growth (FCG); digital image correlation

1. Introduction

Gamma titanium aluminide (γ-TiAl) alloys are emerging as a viable lightweight replacement to nickel superalloys, for use in both the turbine and compressor stages of aero-engines [1,2], as well as in high performance automobiles [3] and the nuclear industry [4]. By mid-2017, the γ-TiAl alloy Ti-48Al-2Cr-2Nb(at.%) has seen 6 years of commercial flight aboard the GEnx engines (General Electric, USA) [1]. Pratt and Whittney, with MTU, is also using the third generation forgeable TNM TiAl alloy in their new geared turbofan engine [1]. For almost three decades, much of the research into these alloys has focused on the low ductility and toughness that limits the tolerance to fatigue crack growth (FCG). This results in a steep slope of the Paris region for FCG when compared to conventional superalloys and steels. In turbines, high cycle fatigue (HCF), where the number of cycles to failure, N_f, is greater than 10^4, is due to aerodynamically induced vibrations at a component's inherent resonant frequencies, as a result of changes in rotational speeds. This HCF therefore exists in addition to the steady state or low-cycle fatigue (LCF - $N_f < 10^4$) loading that occurs upon engine start up and shut down. As a result of the low FCG tolerance, the most promising approach to fatigue lifing for HCF in γ-TiAl alloys has been to operate with stress intensity factors below the FCG threshold, ΔK_{th}, commonly at 50% [5] of

CONTACT T. E. J. Edwards. Email: teje2@cam.ac.uk

the maximum peak cyclic loading stress at which the material can endure 10^7 cycles without failure, known as the run-out strength. Below this stress, the FCG rate should be vanishingly small ($< 10^{-10}$ m cycle^{-1}).

For the next generation of titanium aluminide alloys, higher operational stresses and temperatures, to 750 °C or higher, would enable a significant number of components in commercial aero-engines to be replaced by γ-TiAl alloys [2,6]. To direct the improvement of γ-TiAl alloys for HCF, a complete understanding of the mechanisms by which microstructures resist crack nucleation and growth is required. Similarly, an increased consideration of the complex HCF loading conditions that the component must withstand is required to optimise the texture of γ-TiAl alloy microstructures.

Several reviews of the fatigue properties of γ-TiAl alloys exist [7,8]. However, most of the understanding of fatigue crack growth is focussed on plasticity in the bulk and at crack tips during LCF; HCF is treated using conventional approaches to fatigue life evaluation [9,10]. The present review aims to assess the potential for less conventional methods and considers progress in the understanding of the HCF behaviour of γ-TiAl alloys since ∼2010. This review begins with a brief overview of conventional HCF characterisation of TiAl alloys in section 2, in which the effect of loading and test conditions on the HCF behaviour is discussed. Fatigue crack nucleation mechanisms are covered in section 3. Following this, considerations specific to lamellar γ-TiAl microstructures, such as the orientation of lamellar colonies (i.e. the packets of co-planar α_2-Ti_3Al and γ-TiAl lamellae that are each formed from a single high temperature disordered α-TiAl grain) to the loading axis, and the lamellar thickness, are discussed in section 4. Finally, the possibility for the application of novel test methods to study the HCF behaviour of γ-TiAl alloys down to the nanometre-scale, and with loading procedures that generate deformation fields typical of HCF conditions in industrial applications, will be covered in section 5.

2. Conventional, macroscopic analysis of the HCF behaviour of γ-TiAl alloys

2.1. Damage tolerant design

The Paris law of fatigue crack growth [11] considers the rate of crack growth, da/dN, as a function of the applied stress intensity factor, $\Delta K = K_{\max} - K_{\min}$, according to:

$$\frac{da}{dN} = C_{\mathrm{p}} \Delta K^n \tag{1}$$

where C_{p} is a constant, measured crack-growth coefficient and n is the dimensionless Paris exponent. On a logarithmic plot, Fig. 1, a central, linear section of a sigmoidal FCG dataset exists, beyond the threshold stress intensity ΔK_{th} and before the onset of unstable crack growth at K_{Ic}. The gradient of the straight line fit to this central region equates to the Paris exponent, Fig. 1. The characteristics of the three regions of the Paris curve are shown in Table 1.

For many structural materials in the aero industry, a damage tolerant design is favoured, by which the propagation of cracks occurs but at a sufficiently slow rate for the rate of crack growth to be measured. This requires the slope of the Paris regime of fatigue crack growth to be sufficiently low (∼3 - 5) that changes in the stress intensity factor do not cause a rapid increase in crack growth rate.

	Stage I: Near-threshold	Stage II: Paris regime	Stage III: High-growth rate
Microscopic failure mode	Single shear mechanism	Duplex slip, eventually striations	Various static modes
Crack closure levels	High	Low	-
Load ratio effects	Large	Small	Large
Microstructural effects	Large	Small	Large
Environmental effects	Large	Variable	Small
Near-tip plasticity	$r_c \leq d_g$	$r_c \geq d_g$	$r_c \gg d_g$

Table 1. Characteristics of the three regimes of fatigue crack growth, adapted from [9]. r_c and d_g refer to the cyclic plastic zone size and the grain size, respectively. Due to their high Paris slope, n, γ-TiAl alloys are commonly operated in Stage I, where environmental and microstructural effects on the FCG rate are high. $r_c \approx \frac{1}{\pi}(\frac{\Delta K}{2\sigma_y})^2$ for plane stress loading.

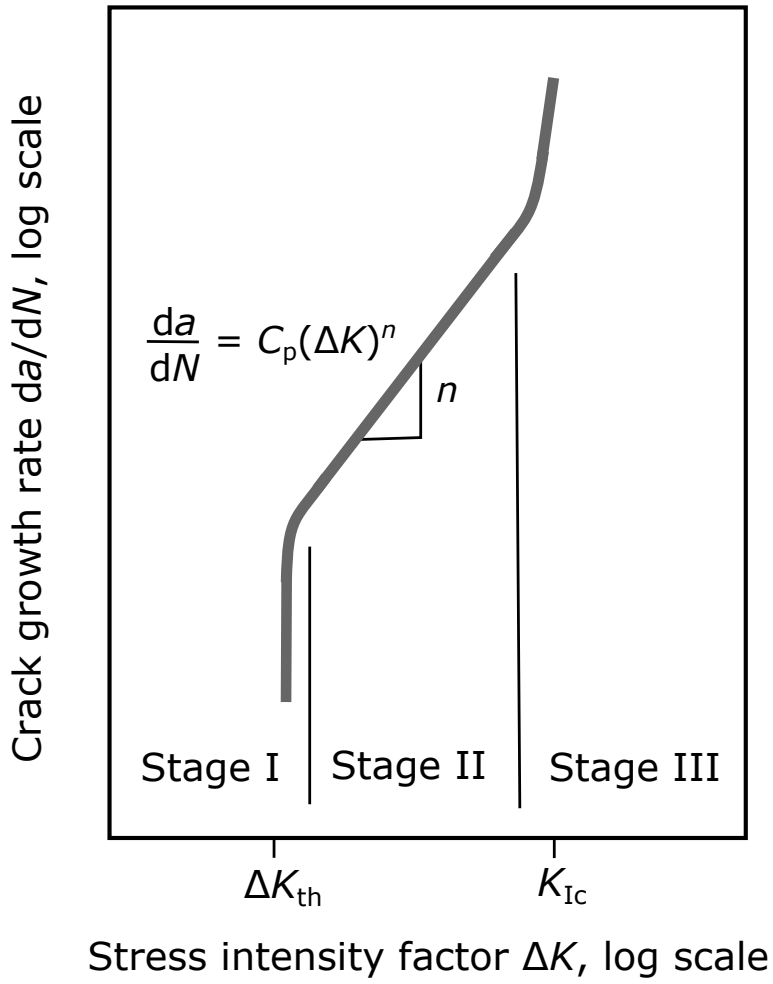

Figure 1. Schematic of fatigue crack growth curves. Adapted and redrawn from [8] (reproduced with permission).

However, titanium aluminide alloys have a Paris exponent of $n \sim 10$ - 50, see Fig. 2, depending on the microstructural condition [12]. This was identified early on for second generation TiAl alloys and complicates their use in the Paris regime, as a 1 MPa $m^{1/2}$ increase in the stress intensity range can cause the crack growth rate to rise by a factor of over 10^2, Fig. 2. The reasons for and the effects of such a high Paris slope are often misunderstood. Indeed, though the Paris slope is often equated to that of engineering ceramics [13], the toughness of lamellar γ-TiAl alloys can reach 30 MPa $m^{1/2}$ - partway between the few MPa $m^{1/2}$ of ceramics and the $\sim$200 MPa $m^{1/2}$ that high strength steels can achieve. The ductility of γ-TiAl alloys is also greater than that of engineering ceramics, being of the order of 1% strain. To better understand the mechanisms behind crack growth in this intermetallic alloy, one should consider the modified Paris law according to Hojo *et al.* [14]. It describes the FCG behaviour of both ductile and very brittle materials by accounting for both the effect of the cyclic stress intensity range and the maximum applied stress intensity:

$$\frac{da}{dN} = C_{\mathrm{p}} \Delta K^p K_{\max}^q \tag{2}$$

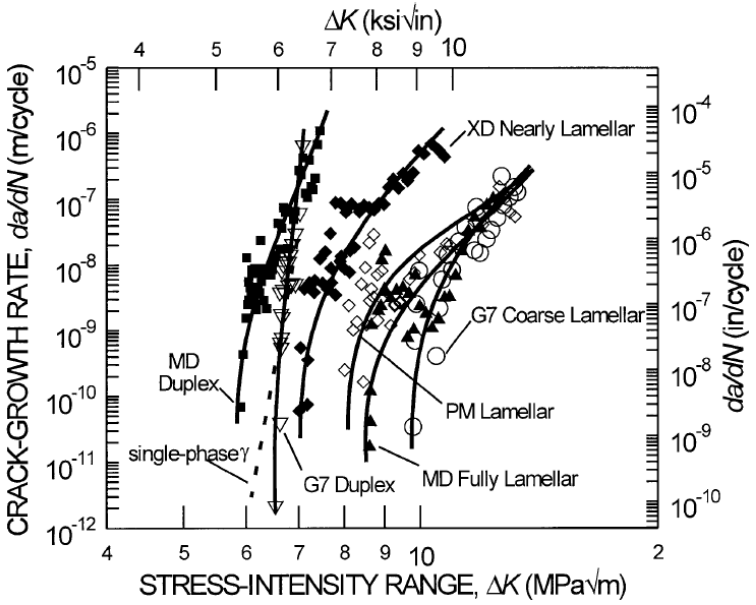

Figure 2. Fatigue crack growth curves for various TiAl alloy microstructures; all have high gradients in Stage II. From [12] (reproduced with permission).

For common engineering metals, $p \gg q$, whereas for toughened ceramics where some cyclic loading may be achieved, $p \ll q$, such that the maximum loading stress is the most damaging aspect of fatigue [15]. Intermetallic materials, such as γ-TiAl alloys, lie somewhere in between, with $p \sim q$, such that values of $n = 50$, obtained by fitting experimental data to the Paris law are gross over-evaluations of the dependence of the FCG rate on the cyclic stress range itself. Filippini *et al.* [16] demonstrated that neither ΔK nor $K_{\max}$ alone can fully describe the FCG properties of Ti-48Al-2Cr-2Nb. Similarly, tests at fixed ΔK on the same alloy by Dahar *et al.* found the Paris slope n to increase with $K_{\max}$ [17], due to static failure modes being activated at higher $K_{\max}$.

Recently, there has been renewed interest in the use of TiAl alloys in the Paris regime, driven by the wish to use the material in the higher temperature parts of the aero-engine [2]. This requires the material to withstand temperatures up to 850 °C [6] and higher stresses. Hence, an improved understanding of, and potential operation within, the crack growth regime (i.e. Stage II) is essential. FCG data of region II fatigue of Ti-48Al-2Mn-2Nb(at.% henceforth) [18,19] shows that both the crack growth prefactor, $C_{\rm p}$, and the Paris slope, n, decrease significantly above 750 °C (the latter to $n = 4$), suggesting that once the ductile-brittle transition is exceeded, damage tolerant design may be achievable if sufficient strength can be maintained. It has been reported that the Paris slope is lower when the lamellae in a TiAl lamellar colony are oriented parallel to the loading axis [20]. Recently, bulk single colony samples have emerged where the orientation of the lamellae can be controlled by the processing method [21], without seeding. This allows components to be produced where the lamellae lie parallel to the loading axis throughout and may result in a further renewed interest in lifing by damage tolerance; this is discussed further in section 4.2.

2.1.1. Effect of the processing method on damage tolerance

Early studies by Gloanec *et al.* [22] on powder metallurgy (PM) consolidation by hot isostatic pressing (HIPping) of γ-TiAl alloys revealed that the fatigue crack growth rate in the Paris regime for the Ti-48Al-2Cr-2Nb alloy was approximately two orders of magnitude higher than the equivalent cast material, even after correction for crack closure. This was attributed to the PM processed material possessing a microstructure of fine equiaxed γ grains that was less able to resist fatigue crack growth compared with the cast, HIPped and heat treated material where coarse lamellar colonies gave rise to a tortuous crack path [22]. Further analysis of this dataset by Zuo *et al.* [23] identified the effective Paris slope (m in section 2.3.1) to be independent of stress ratio and similar between both cast and PM alloys, 8.11 and 8.39 respectively. Rather, it was the C_p prefactor of Paris regime crack growth that was the processing and microstructure-dependent variable [23] and caused the reduction in fatigue behaviour of the PM material. However, this effect was less marked at higher stress ratios where roughness-induced crack closure effects (see section 2.3.1) are less significant.

The development of additive PM processing methods for γ-TiAl alloys has also brought about renewed investigation of fatigue in region II. The application of electron beam melting (EBM) additive manufacturing, a patented advanced powder metallurgy process [24], to second generation Ti-48Al-2Cr-2Nb and third generation Ti-(45-47)Al-8Nb-2Cr (TNB) has enabled near-net shape blade parts to be produced with minimal material wastage compared to cast parts [25]. EBM decreases the porosity and other typical defects compared to casting, and increases the lamellar colony content compared to conventional PM material. This was found to produce superior FCG characteristics, although only the ΔK_th was higher (∼6 MPa $\mathrm{m}^{1/2}$ at a stress ratio $R = 0.05$ for EBM and 5 MPa $\mathrm{m}^{1/2}$ at $R = 0.1$ for PM) and the Paris slopes were similar.

2.2. Stress-life approach

The stress-life (S-N) data compiled by Larsen *et al.* [26] on second generation γ-TiAl alloys indicates that across a range of microstructures, the maximum run-out strength (10^7 cycles), $\sigma_\mathrm{max,th}$, remains above ∼80% of the ultimate tensile stress, σ_UTS. Furthermore, the maximum stress of HCF loading for γ-TiAl alloys can exceed the initial yield stress of the material, irrespective of the stress ratio. This holds even for recent high niobium alloys [27]. Even at target operational temperatures, e.g. 700 °C, the maximum run-out stress is at least 70% of the ultimate tensile strength, as a result of a decreased yield strength and increased ductility, at high temperatures, without any substantial change to the work hardening behaviour. This indicates that some degree of plastic cycling must occur in TiAl alloys cycled at the maximum run-out stress across the temperature range, as they are loaded above the elastic limit. This will be discussed further in section 5.1.

The emergence of giga-cycle test methods [28,29] has meant that S-N measurements are no longer limited to 10^7 cycles; 10^{10} is now commonly achievable. Testing of the alloy Ti-45Al-10Nb [30,31] revealed that by 10^8 cycles at a stress ratio of 0.1, an endurance limit was reached, although this is not seen in samples tested at $R = 0.5$ which lasted for 10^{10} cycles, Fig. 3. Considering the nature of HCF by resonant vibrations in turbine blades which are already experiencing a steady state centrifugal load, the apparent absence of an endurance limit even by 10^{10} cycles at high R is prohibitive to conservative lifing to a stress well below a run-out value.

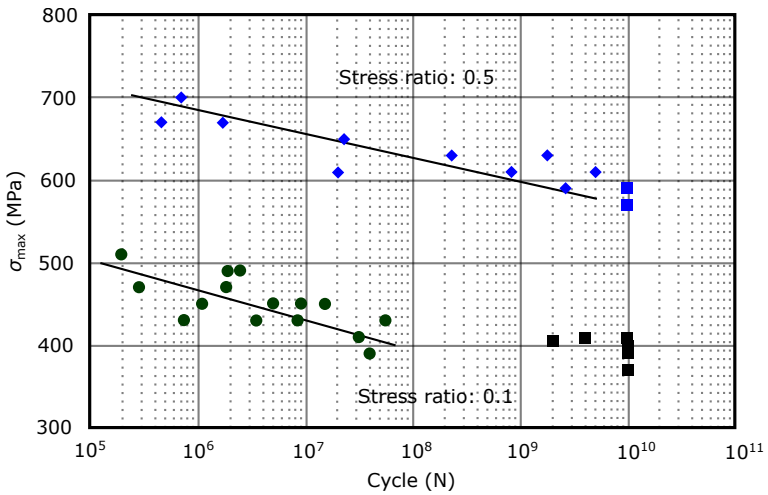

Figure 3. Gigacycle fatigue S-N of Ti-45Al-10Nb. Redrawn from [31] (reproduced with permission).

2.3. Fatigue crack growth threshold

The standard method for determining the FCG characteristics of γ-TiAl alloys has been to test at a frequency of 20 Hz and a stress ratio $R = 0.1$, with progressive load shedding to measure the threshold stress intensity according to ASTM standard E647 [10]. Features of conventional fatigue threshold measurements commonly encountered on γ-TiAl alloys, such as stress ratio dependence and small crack effects, are discussed in the following sub-sections.

2.3.1. Crack closure

The dependence of the fatigue threshold on the stress ratio, $R = \sigma_{\min}/\sigma_{\max}$, for γ-TiAl alloys can be accounted for by considering the possibility for crack closure effects, first proposed by Elber [32]. For each stress intensity range ΔK an effective range ΔK_{eff} is considered in the Paris law treatment [9,33]:

$$\frac{da}{dN} = C_{\text{p}}\Delta K_{\text{eff}}^{m} \text{ with } \Delta K_{\text{eff}} = K_{\max} - K_{\text{op}} = \mathbf{U}\Delta K \tag{3}$$

where $m = p + q$, $\mathbf{U}$ is a material-dependent function that depends mainly on R and $K_{\max}$, and K_{op} is the stress intensity factor at which a crack opens fully. K_{cl} is the stress intensity at which the crack begins to make closure contact upon unloading and in practice $K_{\text{cl}} \approx K_{\text{op}}$ [9]; this occurs at a critical stress ratio $R = R_{\text{cr}}$. The dependence of the fatigue crack threshold ΔK_{th} on R resulting from crack closure can further be accounted for to produce an effective fatigue crack threshold, $\Delta K_{\text{th,eff}}$, which is independent of R and a material property [34], according to:

$$\begin{aligned} &\text{for} \quad R < R_{\text{cr}},\ K_{\min} < K_{\text{cl}} \text{ and } K_{\max} = \frac{\Delta K_{\text{th}}}{1-R} = K_{\text{cl}} + \Delta K_{\text{th,eff}} \\ &\text{for} \quad R \geq R_{\text{cr}},\ K_{\min} \geq K_{\text{cl}} \text{ and } \Delta K_{\text{th}} = \Delta K_{\text{th,eff}} \end{aligned}$$

Hénaff *et al.* [35] applied this model to a near-γ alloy. They demonstrated that the

function **U** was approximately constant across the ΔK range of testing in both air and vacuum at room temperature. The environment therefore interacts only weakly with the crack at this temperature and K_{op} is constant. Similar results were obtained on lamellar and duplex structures [36]. The reasons for crack closure can be diverse [9] and are material dependent [15]. The extrinsic and intrinsic processes occurring at a crack tip loaded in fatigue for metals, intermetallics and ceramics are summarised in Fig. 4. For γ-TiAl, roughness-induced closure appears to be a key mechanism for lamellar microstructures, where tortuous translamellar crack deflection results in a serrated fracture surface, particularly for larger colony sizes [17]. Roughness-induced crack closure does not occur in lamellar γ-TiAl alloys for stress ratios above ∼0.5, and also in the cases of near-γ and duplex structures where smooth fracture surfaces cause only crack tip plasticity, not roughness, to bring the crack surfaces into contact sooner [35]. If fretting occurs alongside oxidation of the crack surfaces, then an improvement in the near-threshold fatigue properties is found at 800 °C, which are better than those at both 25 °C and 600 °C [37,38].

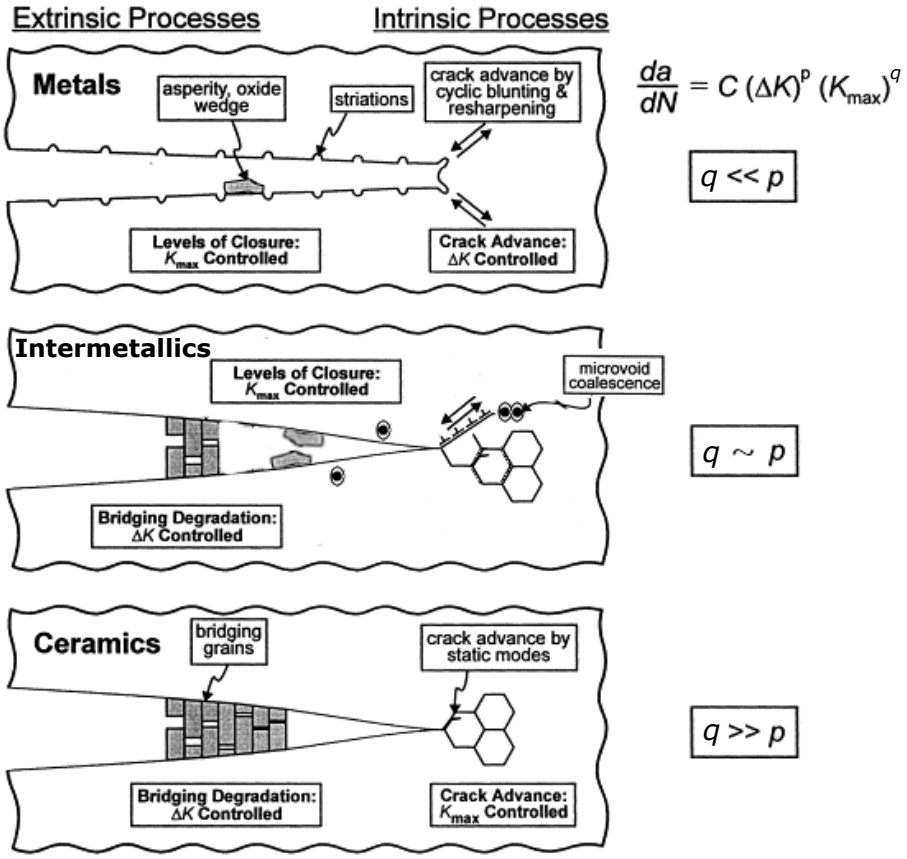

Figure 4. Mechanisms for fatigue crack growth in intermetallics, compared with those present in metals and ceramics. Extrinsic toughening in intermetallics may be achieved by grains bridging cracks, such as bridging lamellae in lamellar γ-TiAl alloys. In ceramics and intermetallic composites, crack bridging may additionally involve strong and stiff fibres, or elongated metallic grains that undergo ductile rupture [15]. Ahead of the crack in γ-TiAl intermetallics, crack growth may occur by cleavage fracture along fatigue cycled slip planes, and by coalescence of microcracks ahead of the crack tip; static fracture modes also occur. Microcrack/microvoid toughening occurs in the proximity of cracks. Adapted from [15] (reproduced with permission).

2.3.2. Small cracks

Since the early 1990s, it has been recognised [39] that small cracks ($< \sim$1 mm) are of particular concern in the fatigue of γ-TiAl alloys. Indeed, the concept of a threshold stress intensity range ΔK_{th} below which crack growth is vanishingly low ($< 10^{-10}$ m cycle^{-1}) occurs only for long cracks, which obey linear elastic fracture mechanics (LEFM). However, short cracks have been observed to propagate in γ-TiAl alloys at stress intensity factors below the ΔK_{th} determined for long cracks, and at rates which are several orders of magnitude faster than predicted using stress states inferred from LEFM [39]. The conservative design limit for fatigue protection using ΔK_{th} is therefore not useful for short cracks. The reason for this effect has been demonstrated in a study of 25 - 500 µm surface cracks performed by Kruzic *et al.* [40], building on preliminary work by Chan and Shih [41]. This identified small crack growth by cleavage cracking along colony and interlamellar boundaries, as well as low-index crystallographic planes within lamellae and equiaxed grains. An abundance of crack-deflecting interfaces in the lamellar structure appears to place no lower limit on the stress intensity range for short crack propagation in the early stages of crack growth. However, cracking in duplex γ-TiAl appears to stop below ΔK_{th}, when using the effective $\Delta K_{\mathrm{th,eff}}$, which is corrected for crack closure. This makes the duplex microstructure attractive for engineering applications.

The difficulties caused by the presence of small cracks in γ-TiAl alloys have been studied more recently by introducing micro-scale notches in globular γ grains, or at their boundaries, and in lamellar colonies with specific orientations to the loading axis [42–45]. The FCG rate of several tens of small cracks, some emanating from the micro-notches, some not, were tracked across microstructural barriers. Three stages of short crack growth were identified, Fig. 5. Firstly, the cracks that lie within the colony of initiation. Secondly, the cracks stretching into the neighbouring colony ahead. Finally, the physically short cracks that grow without closure and develop into stage II FCG, behaving as long cracks until they are temporarily arrested by another microstructural barrier (grain or colony boundaries). The progression of all small cracks through these stages led the authors to suggest that it is the minimum stress intensity range for surpassing the first significant microstructural barrier, generally a colony boundary in fully lamellar microstructures, that should be considered for component design and lifing. Indeed, above this stress intensity range, the small cracks grew rapidly, see the minimum in FCG rate arrowed in Fig. 5. For most of the alloys investigated, this threshold was approximately half that determined from long crack growth that is usually used for lifing [5].

An alternative useful approach to accounting for the presence of small cracks in γ-TiAl alloys is that of Filippini *et al.* [16,46], where the El-Haddad model modified by Tanaka *et al.* [47] was applied. This combines the stress-life and damage-tolerant (FCG) approaches to fatigue by the intermediate of an inherent minimum flaw size, which has previously been related to the concept of small cracks [9]. The intrinsic fatigue stress intensity range threshold was determined from compact-tension specimens and the maximum run-out stress values were determined from plain cylindrical specimens with and without EDM-introduced artificial defects, at room temperature and 700 °C. Both the Ti-48Al-2Cr-2Nb and TNB alloys were found to obey the same Tanaka law, Fig. 6, despite different strengths and colony sizes. A similar percentage of lamellar colonies were produced in both alloys through electron beam melt processing. This parameter, the volume fraction of lamellar colonies, was therefore reported to dominate the HCF properties of γ-TiAl alloys.

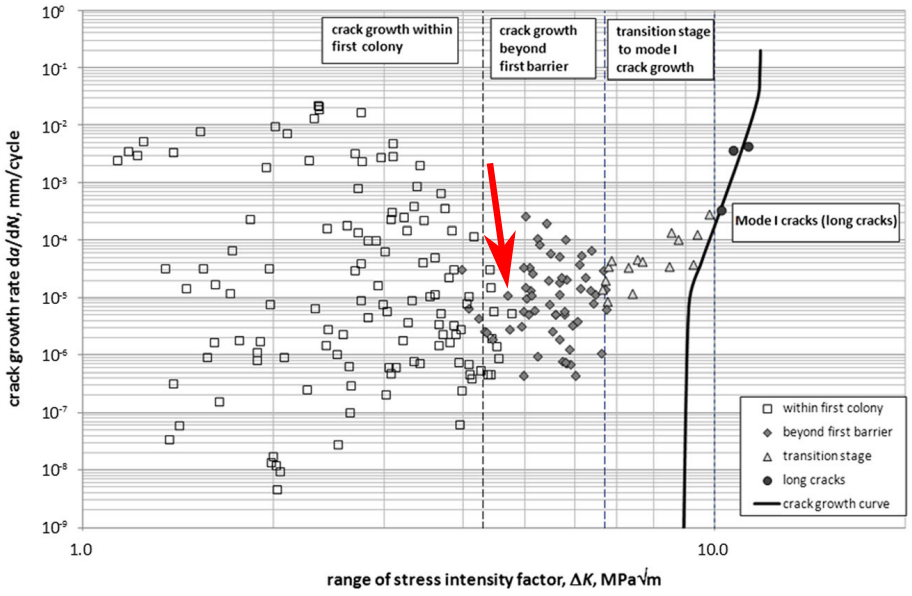

Figure 5. Small crack growth rates in TiAl alloy TNM-B1, with the minimum in FCG rate at the first microstructural barrier arrowed in red. Adapted from [45] (reproduced with permission).

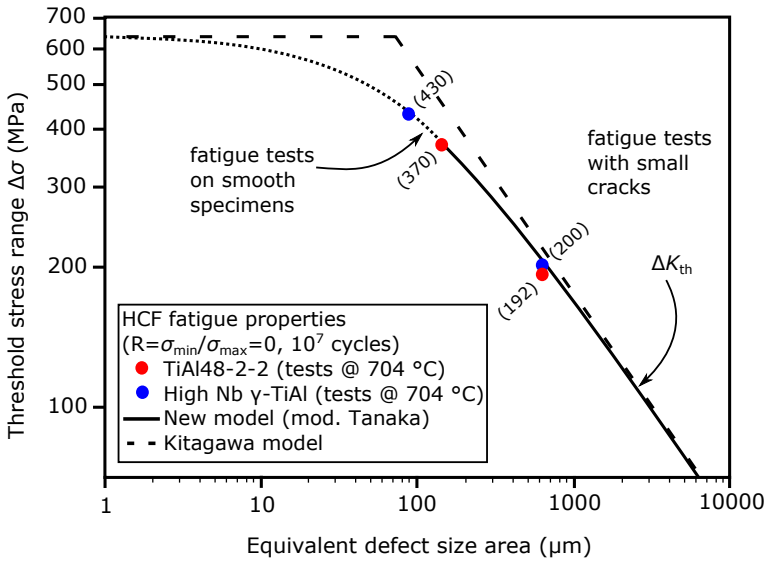

Figure 6. Kitagawa-Takahashi diagram for electron beam melting processed TiAl alloys. Redrawn and adapted from [46] (reproduced with permission).

2.4. Object damage

In addition to understanding the material parameters for design against fatigue failure due to flaws inherent to the production of TiAl components, it is necessary to understand the size of flaws that might be generated by object damage (foreign or domestic) during engine operation. There are relatively few published studies concerning object damage of γ-TiAl alloys. Early studies by Harding and Jones [48] employed quasi-static and low-speed drop indentations. Ballistic impact testing by Draper et al. [49,50] using a gas gun to project small steel spheres at aerofoil-shaped specimens determined the impact energy to be the dominant factor in characterising crack formation. The range

of impact energies was 0.2 to 2.0 J. Where the damage exceeded the microstructural dimension (i.e. the lamellar colony size), a straightforward FCG threshold analysis of the crack length suitably predicted the measured reduction in fatigue strength [50]. Attempts to model this behaviour with a finite element model [51] identified that a lower amount of ductility occurred before crack formation in ballistic testing (1 - 2% plastic strain) compared with static indents (2 - 3% plastic strain).

More recently, Draper et al. have extended their study to third generation γ-TiAl alloys [52]. The GMPX alloy Ti-45Al-5Nb-0.2C-0.2B displayed no improvement in the remnant fatigue strength after impact testing compared with older generation alloys such as Ti-48Al-2Cr-2Nb, hence calling into question the suitability of third generation γ-TiAl alloys for higher strength aero-engine blade applications. Bache and Morgans [53] have undertaken simulated object damage of Ti-46Al-8Ta at much higher impact energies, and using cube-shaped steel projectiles. Damage was often brittle, with surface chips ejected, and deep macroscopic cracks (> 1 mm) surrounding the damage sites. Further HCF of the damaged specimens at $R = 0.1$ with an increasing $\sigma_{\max}$ until failure found that comparable HCF endurance strengths were achieved at 20 °C and 650 °C, although only a few samples were tested and up to a maximum of 10^5 cycles. A plateau in fatigue strength was reached beyond an impact energy of ∼2.4 J, which suggests there exists a maximum flaw size to engineer for; however, complete specimen failure occurred upon an impact energy of 9.8 J.

2.5. Effect of temperature and environment

The effect of temperature on the fatigue threshold properties of γ-TiAl alloys has been reviewed extensively elsewhere [7,8]; however, little further progress has been made since towards understanding the effect of temperature on the micromechanisms of fatigue crack initiation and growth [27,54–59]. The effect of temperature appears to be complex. For instance, although the failure mechanism of brittle trans- and inter-lamellar fracture is unchanged from 25 to 800 °C, the alloy Ti-47.7Al-1.9Nb-0.9Mn + 1 vol.% TiB_2 has a higher threshold stress intensity factor in air at 25 °C and 800 °C than it does at 600 °C [38], Fig. 7(a). In a similar study [60] of FCG rates at fixed stress intensity across the same temperature range on Ti-46.5Al-3Nb-2Cr-0.2W, Fig. 7(b), the mechanisms involved were thought to be associated with both increased ductility upon heating, and also increased environmental embrittlement in the crack region, which nominally decreases fatigue life. Growth rates are several orders of magnitude higher in air than in a vacuum [61]. However, up to 600 °C, oxide formation is rarely reported, suggesting that oxidation-induced crack closure is not significant. An alternative mechanism for environmental embrittlement is by hydrogen uptake from water vapour. This occurs in iron aluminides [61], though the mechanism behind the temperature dependence of this is not well understood. Elsewhere, strain ageing effects in the 400 °C to 650 °C range may reduce crack tip plasticity due to increased dislocation pinning by Ti_{Al} + V_{Ti}, an antisite & vacancy pair, which has a negative strain-rate dependence [8].

3. Fatigue crack nucleation mechanisms in γ-TiAl alloys

In situ SEM observations have found that cracks in γ-TiAl alloys initiate in fatigue during the latter stages of HCF life, generally within the final 10 % of the lifetime [62]. However, acoustic emission measurements have found that even within the first loading

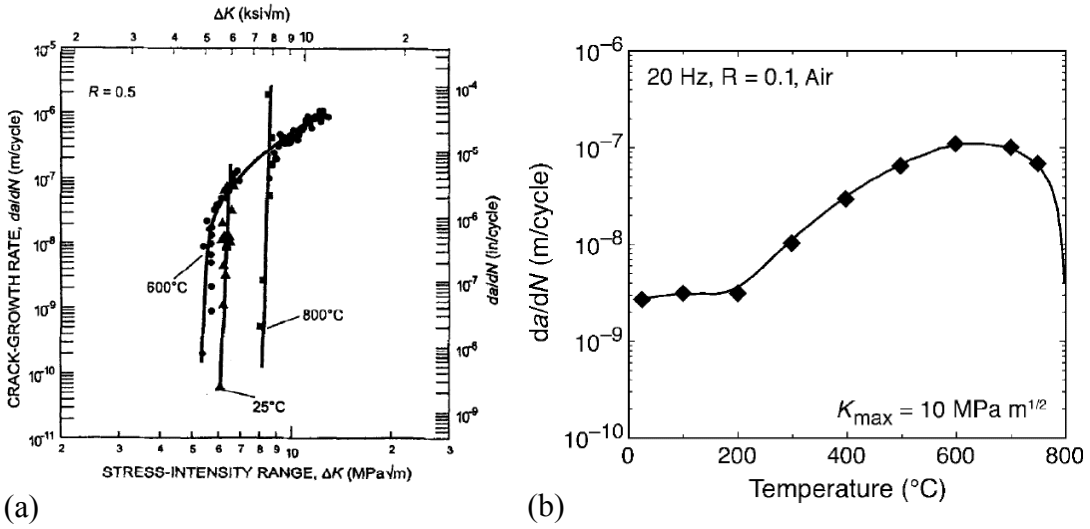

Figure 7. Effect of temperature on FCG behaviour. (a) from [38] and (b) from [60] (reproduced with permission).

cycle microcracking can initiate [63,64]. There is evidence [8,65] that the growth of fatigue cracks in γ-TiAl alloys operates by the formation of microcracks ahead of the growing crack. This can be seen as many crack initiation events that link up by more ductile-type translamellar rupture. Further, the initiation of cracks has been observed *in situ* on electropolished surfaces, where no flaws were apparent, although laser ablation-formed micro-notches elsewhere on the surface remained inactive [45]. From this evident complexity and preponderance of crack initiation in the HCF failure of γ-TiAl alloys, it is clear that understanding the mechanisms for crack nucleation is crucial to optimising the HCF properties.

The nearly flat *S-N* curve that is commonly reported for γ-TiAl alloys has been shown by Jha *et al.* [66] and elsewhere [67] to be characteristic of crack initiation both at the surfaces, and in the bulk. In itself, this distinction of flaw location is not novel. Weibull statistics have been used on brittle materials to demonstrate these two regimes [68]. The further consideration for γ-TiAl alloys is whether the mechanism of initiation is different. Although crack nucleation is common at internal inclusions and pores in ductile engineering alloys in the gigacycle regime [29], cracks in gigacycle fatigue tests of more brittle γ-TiAl alloys were also identified to be volume initiated [31]. This was in particular at γ/α_2 interfaces and was attributed to plastic incompatibility.

At a surface, fatigue cracks may form by the extrusion of soft-mode oriented lamellae (where the angle of the lamellar interface to the loading axis, Φ, see Fig. 8, lies between 15° and 75°) by plasticity in the γ-TiAl phase parallel to the lamellar interfaces, known as longitudinal plasticity [69,70]. This is an initiation mechanism commonly found in ductile systems [9] and requires the local critical resolved shear stress to be exceeded. In the bulk, this mechanism may be resisted by the constraint of the surrounding colonies [71]. Nevertheless, deformation twinning in the γ-TiAl phase can generate grain boundary decohesion at a free surface in equiaxed γ and lamellar microstructures [72,73]. Ahead of static and fatigue cracks in lamellar structures, transverse twinning in the γ-TiAl phase causes lamellar interfaces to debond [65,74].

Another crack initiation mechanism in the bulk is that defined by Cottrell [75], whereby in semi-brittle crystals, the intersection of slip planes can form an obstacle

to slip, and a brittle-type crack nucleates at the obstacle. This occurs when the elastic energy accumulated there by dislocation pile-up is sufficient to drive the formation of the free surfaces of a crack. This mechanism is thought to nucleate microcracks identified by TEM along the low energy $\{111\}_\gamma$ cleavage planes at the intersection between the easy operating longitudinal slip systems and the Hall-Petch strengthened transverse slip systems in lamellar γ-TiAl microstructures [76–78]. In this sense, globular, non-lamellar, γ grains in nearly lamellar TiAl microstructures may initiate microcracks as the lack of lamellar interface strengthening permits relatively unimpeded slip on multiple planes. Hence significant pile-up forces at intersection obstacles may arise. This has not been extensively investigated.

A final crack initiation mechanism in lamellar structures is decohesion of lamellae oriented perpendicular to the loading axis ($\Phi = 90°$) [64,79]. The scale of cracking achievable before any microstructural barrier is met, and the regularity of the occurrence of this initiation mechanism, strongly suggests action should be taken to either strengthen the lamellar interfaces, reduce the colony size to limit the spatial extent of damage, or avoid such colony orientations altogether.

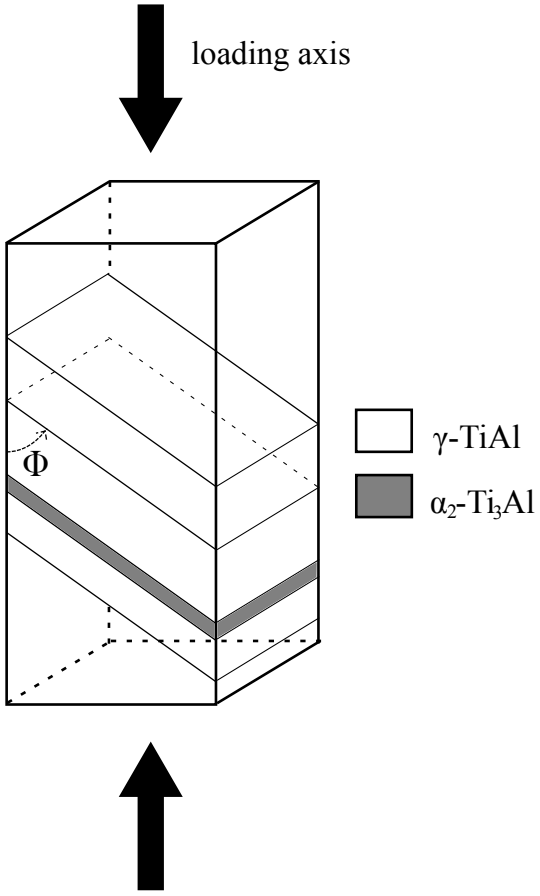

Figure 8. Schematic of a cuboidal PST (single colony) lamellar TiAl specimen with the angle Φ of the lamellar planes to the vertical loading axis indicated.

Crack initiation in the latest generation high Nb alloys in both quasi-static and fatigue loading [80,81] also involves the retained ordered β_0-TiAl with brittle ω-Ti phase precipitates that concentrate stress. This becomes particularly problematic when the β_0 phase covers large amounts of lamellar colony boundaries, such that extensive micro-

crack nucleation in β_0/ω may result in extended planes of coalescing flaws. Improved thermodynamic stabilisation of the β_0 phase is required to avoid this.

4. Lamellar TiAl-specific considerations for crack growth in HCF

4.1. Microstructural dimensions appropriate to HCF characterisation

Classically, the γ grain size, or in the case of lamellar γ-TiAl alloys, the colony size, is the main microstructural dimension investigated towards optimising HCF properties. This is then supplemented by a consideration of the proportion of equiaxed γ grains vs lamellar colonies, the fatigue threshold generally increasing with decreasing equiaxed γ content [82], Fig. 9. The size of lamellar colonies influences the FCG rate as smaller colonies have a high density of colony boundaries. Hence cracks only propagate a small distance before being deflected at a boundary. However, as Dahar *et al.* [17] have pointed out, a large colony size maintains a cyclic crack tip plastic zone within the colony of initiation for as long as possible in the near-threshold regime. Hence, by not exceeding stage I type growth, surface roughness-induced crack closure is encouraged by the single-slip-like behaviour [83]. Therefore, although a finer microstructure limits initial crack propagation, once a short crack attains the size of several colonies, it acts as a long crack, where the presence of many weak colony boundary interfaces facilitates crack propagation [36]. It seems generally agreed that the optimum colony size is in the 50 - 100 µm range for several second and third generation γ-TiAl alloys [84,85]. In fact, according to Filippini *et al.* [46], the intrinsic effective threshold stress intensity range is a material property that cannot be much affected by grain size, as crack growth at the limiting rates for the application of γ-TiAl alloys is very much sub-granular.

In lamellar γ-TiAl alloys, the microstructure is rarely considered in terms of the lamellar thickness with regards to HCF properties. It was generally thought that the lamellar thickness is related to lamellar colony size, being proportional to its square root [86]. Based on quasi-static toughness measurements alone, the influence of lamellar thickness is unclear: several studies [87,88] indicate that lamellar refinement increases fracture toughness, whilst another [89] found no such relationship to exist. This was possibly due to the variation of the colony size in these studies. However, a systematic study by Cao *et al.* [90] employing multistage cooling strategies demonstrated that the colony size and lamellar thickness can be varied independently, over several orders of magnitude. This method was adopted by Mine *et al.* [91] to produce polycrystalline single edge micro-notched specimens with lamellar thicknesses of 0.91 µm and 3.8 µm, for a range of colony sizes. Materials with refined lamellae had lower fatigue crack growth rates than those with thick lamellae. This was attributed to the high degree of microcracking in neighbouring lamellae ahead of the crack tip in the refined material. Once linked, such microcracking led to heavily roughened crack faces, and hence increased closure. In material containing thicker lamellae there is not as much microcracking [92]. However, the wider bridging ligaments when microcracking does occur give rise to increased scatter in HCF behaviour compared with the refined lamellae condition. In contrast, Chan and Kim [87,88] found that refining the lamellae was associated with an increase in the resistance to translamellar microcracking. Plasticity upon fatigue loading generates transverse twins and slip bands that are known to be preferred propagation paths [77]. The CRSS of such transverse deformation mechanisms is dependent on lamellar thickness (Hall-Petch effect [90]) and composition; this

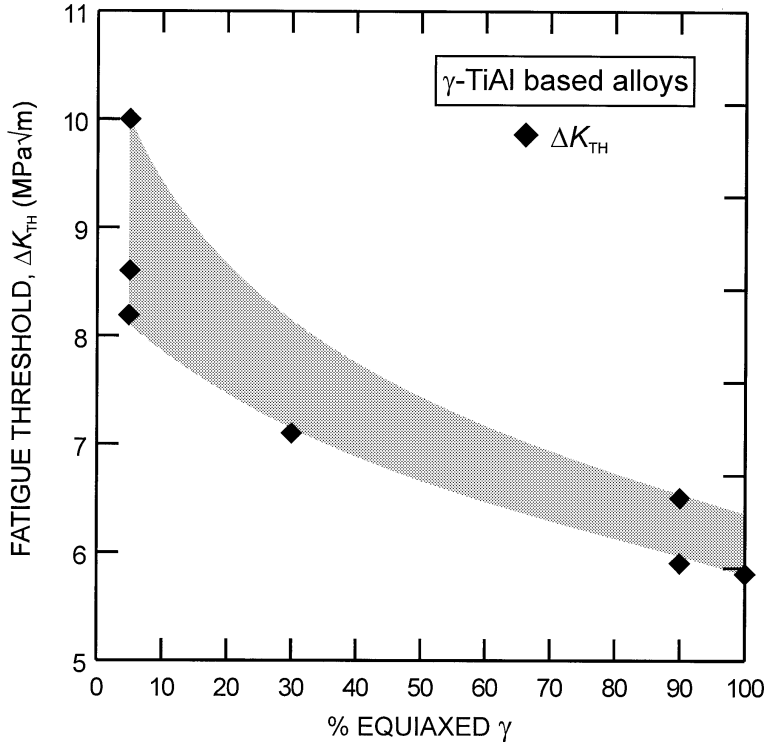

Figure 9. Effect of the equiaxed γ content on the measured fatigue threshold. From [82] (reproduced with permission).

may explain the above discrepancies. Compositional differences between the studies may have also influenced the ease of debonding lamellar interfaces. A decreasing Al content has been demonstrated to refine the lamellar thickness, as well as reducing the in-plane γ domain length, for equivalent processing conditions [93,94]. Under LCF conditions, Umakoshi *et al.* [69] found the strengthening of this domain length refinement to resist longitudinal plasticity, which otherwise causes the formation of surface micro-extrusions of lamellae that act as micro-crack nucleators, as evoked in section 3.

Finally, long term thermal exposure of Ti-45Al-2Mn-2Nb-0.8 vol.%TiB_2 at 700 °C for periods of up to 10 000 h [95,96] was found to improve the maximum fatigue strength at run-out by almost 100 MPa, but only beyond 6 000 h of exposure. Appropriate variations in test-piece production methods showed that this apparent strengthening did not result from surface healing effects, but rather from stress relaxation in the bulk; the dominant microstructural change evident from imaging was simply transformation of the α_2 phase to γ and hence a thinning of the α_2 lamellae. This suggests that increasing the volume fraction of γ phase, presumably bringing this closer to the thermodynamic equilibrium, might improve the stress-life properties of lamellar γ-TiAl alloys.

4.2. Fatigue of polysynthetically-twinned (PST) crystals

Polysynthetically twinned (PST) crystals were used to study the mechanical properties of lamellar γ-TiAl alloys, mostly in Japan in the 1990s and early 2000s [69,97,98]. Samples were grown using a floating zone technique with either seeding or initial narrowing of the floating zone to produce a single α phase grain that transforms to a single

stack of γ-TiAl/α_2-Ti_3Al lamellae, effectively a single lamellar colony, upon cooling. The majority of data collected concerned monotonic loading and strain-controlled low cycle fatigue across the temperature range, as the study of plasticity mechanisms and the effect of the anisotropy caused by lamellar orientation to the loading axis, Φ, was the focus. An extensive review by Umakoshi *et al.* [69], Fig. 10, nevertheless provides some insight as to optimum lamellar orientations for HCF testing: $\Phi = 0°$ performs better than $\Phi = 45°$, mainly due to the reduced strength of the $\Phi = 45°$ orientation.

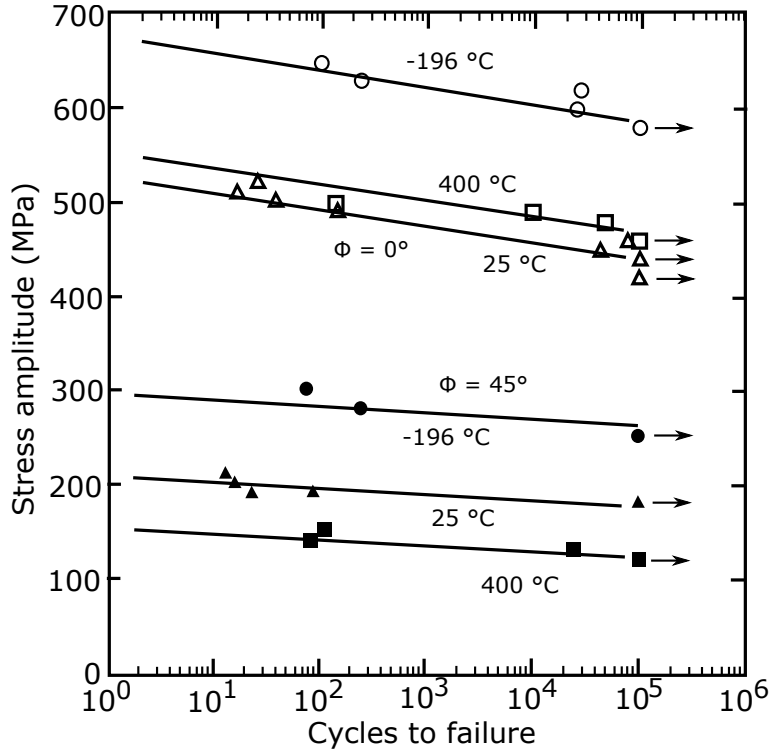

Figure 10. Stress-life testing of PST crystals. From [69] (reproduced with permission).

An alternative to growing bulk PST crystals is to produce micromechanical testpieces from individual lamellar colonies by selective machining. This has been achieved on TiAl alloys by micro-electro-discharge machining (μEDM) [99] and focussed ion-beam milling (FIB) [99–103]. It has enabled the critical resolved shear stress of deformation mechanisms to be measured, that might not otherwise be individually activated, e.g. twinning of γ-TiAl. However, studies to date have been limited to monotonic testing between 25 Celsius [99–102] and 700 Celsius [103]. It is possible for in-situ SEM measurements of stable crack growth to be made with micromechanical methods [104]. However, for meaningful fatigue crack growth data to be achieved, the plastic zone should be considerably smaller than the testpiece dimensions, and though this is achievable for brittle ceramics [104], the plastic zone radius of γ-TiAl alloys in fatigue is several microns [105], which is at the limit for a micromechanical testpiece.

An intermediate between PST crystals, Fig. 11(a), and equiaxed, atextured polycrystalline microstructures is a columnar microstructure. For lamellar γ-TiAl alloys, there are two types of columnar grained structures that can be developed that have a same Φ in all colonies [106]. The first have the lamellar planes of neighbouring colonies almost parallel to each other, Fig. 11(b), the second only have equal tilt angles of the lamellar planes to the axis of the columnar growth, Fig. 11(c). Multiple

groups [107–110], mainly based in China, have pursued the directional solidification route on application-relevant alloy compositions to develop such columnar microstructures. Control of lamellar orientations was achieved by varying the extraction rate from a Bridgman-type furnace [107], and employing different α- or β-Ti [110] seeding techniques and multiple re-solidification [108]. Limited fatigue testing of such microstructures has been undertaken by both S-N [111] and compact-tension FCG [112] methods. For testing of $\Phi = 0^\circ$ and $\Phi = 90^\circ$ lamellar orientations, the closure-corrected fatigue threshold was identified to be equal in both cases, at ∼5 MPa $m^{1/2}$, but the Paris slope was much lower in the $\Phi = 0^\circ$ case ($m \sim 5$, vs. $m \sim 32$ for $\Phi = 90^\circ$); this is consistent with increased ductility and the impossibility for growth of the primary crack along lamellar interfaces in the $\Phi = 0^\circ$ case.

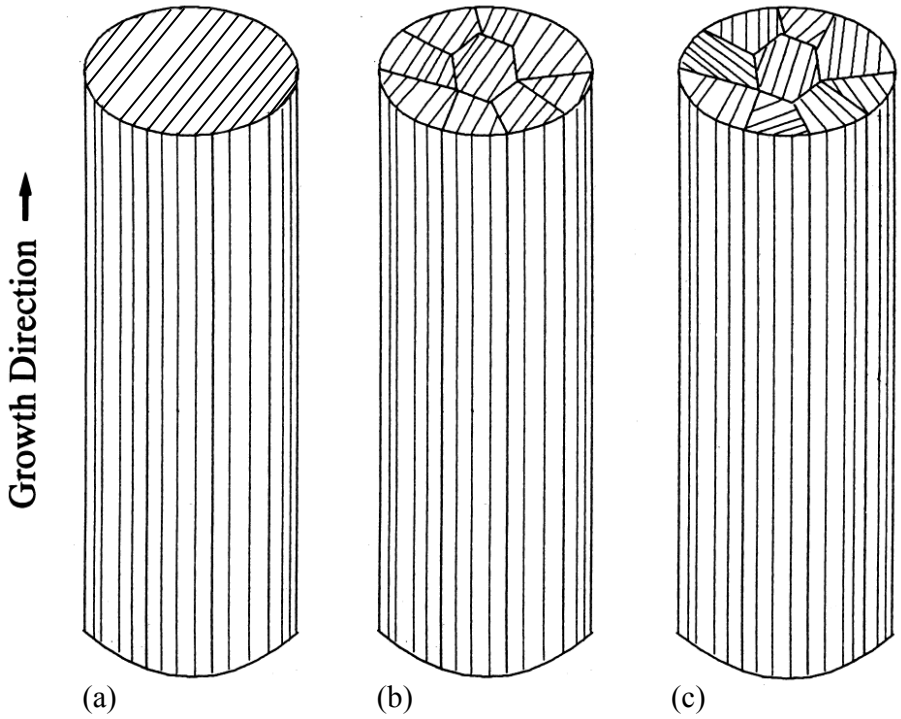

Figure 11. Potential microstructural variety in directionally solidified crystals with the same Φ angle: (a) polysynthetically twinned crystal, PST, (b) columnar grains, approximately co-planar lamellar interfaces, (c) columnar grains, non-coplanar lamellar interfaces, but same Φ angle in every grain. In the present example, $\Phi \sim 0^\circ$. Adapted from [106] (reproduced with permission).

The culmination of such directional solidification endeavours enabled Chen *et al.* [21,113] to produce macroscopic PST crystals of Ti-45Al-8Nb several tens of millimetres long. The lamellar orientation was determined by the extraction rate from the Bridgman furnace, and not by prior seeding. The measured monotonic strength was high for the alloy system, and ductility reached 7% in the $\Phi = 0^\circ$ orientation at room temperature. This method has potential for the mass production of effectively single crystal turbine blades, similarly to the single crystal nickel superalloy counterpart [114]. As expected, the creep strength was considerable [21]; however, data on the HCF behaviour are yet to appear.

Unfortunately, the optimum microstructure for high strength high cycle fatigue properties, combined with a tolerance for fatigue crack growth, is unclear. Within the context of preferentially oriented lamellar microstructures alone, there is no evidence

as to whether columnar grains or PST, Fig. 11, will perform better. From the absence of colony boundaries in PST crystals, their creep properties are likely to outperform their columnar-grained counterparts for the same composition and lamellar thickness. Failure by delamination at the free surfaces is known to occur from the machining of lamellar TiAl alloys [115], but is rarely investigated in the context of HCF. The varied combinations of mechanical loading - tension, torsion, bending - experienced by a component in fatigue may induce such delamination. Hence the possibility for a choice of orientations of the columnar grains could locally increase resistance to this failure mode, whereas PST crystals have no such flexibility (e.g. maintaining $\Phi = 0°$, but changing the twist angle of the lamellae about the blade axis, Fig. 11(c)).

4.3. Fatigue cracking of specific colony orientations in polycrystals

Studies on PST crystals have highlighted the impact of lamellar orientation on the fatigue behaviour of lamellar TiAl alloys and the potential for the production of components from an optimum orientation. However, the majority of developmental and applied alloys are polycrystalline. Throughout the 1990s and 2000s there was a considerable drive to develop compositions and processing methods that resulted in texture-free microstructures [116], where a growing fatigue crack is therefore likely to encounter all possible colony orientations. The growth of PST crystals from arbitrary TiAl compositions to produce fatigue testpieces with a variety of lamellar orientations is a complex and onerous task. Further, it does not enable the study of changing lamellar orientations across colony boundaries on the fatigue crack growth. Quite simply, PST crystals do not contain colony boundaries.

Over recent years, this has inspired efforts to establish the HCF properties of individual lamellar colonies in polycrystalline samples by the careful positioning of EDM or diamond wire pre-cracks [17,62,78,117]. The measurement of ΔK_{th} of Ti-46Al-8Nb for lamellar orientations Φ of 0 to 75° at 650 °C [117] determined the most FCG resistant orientation in the near-threshold regime to be $\Phi \sim 0°$, Fig. 12(a). The colony orientations with the lowest threshold values were those where $\Phi = 40$ - $65°$, i.e. the softest orientations in PST studies [97]. The secondary orientation, Ψ, of the lamellar planes with respect to the advancing crack front, had no marked effect: lamellar planes at $\Phi \sim 0°$ lying parallel to the crack front, or perpendicular, yielded equal ΔK_{th} values. Translamellar fracture was the dominant fracture mode for the majority of colony orientations, except for those close to $\Phi = 90°$, where interlamellar debonding occurred. Hence, understanding what causes the lamellae to crack transversally is paramount. The similarity between the U-shaped ΔK_{th} vs. Φ in Fig. 12(b) and that identified for the yield stress of PST crystals against Φ in compression, Fig. 12(a), suggests that the development of extensive longitudinal plasticity in the softest lamellar orientations causes the opening of micro-cracks where this intersects active transverse slip/twinning, i.e. the Cottrell mechanism detailed in section 3. In principle, transverse deformation mechanisms are less likely to cause micro-crack formation at transverse-transverse intersections as the extent of plastic strain generated on these systems is lower [102]. This correlates well with the highest ΔK_{th} being at $\Phi \sim 0°$, where the Schmid factor is very low for longitudinal mechanisms. Further, in-situ SEM high temperature (750 °C) HCF loading of Ti-45Al-8Nb-0.2W-0.2B-0.1Y found the development of longitudinal plasticity in soft-mode oriented colonies caused colony boundary cracking at the ends of lamellae [62].

In another study [78], the fatigue cracking mechanism of lamellar colonies of Ti-

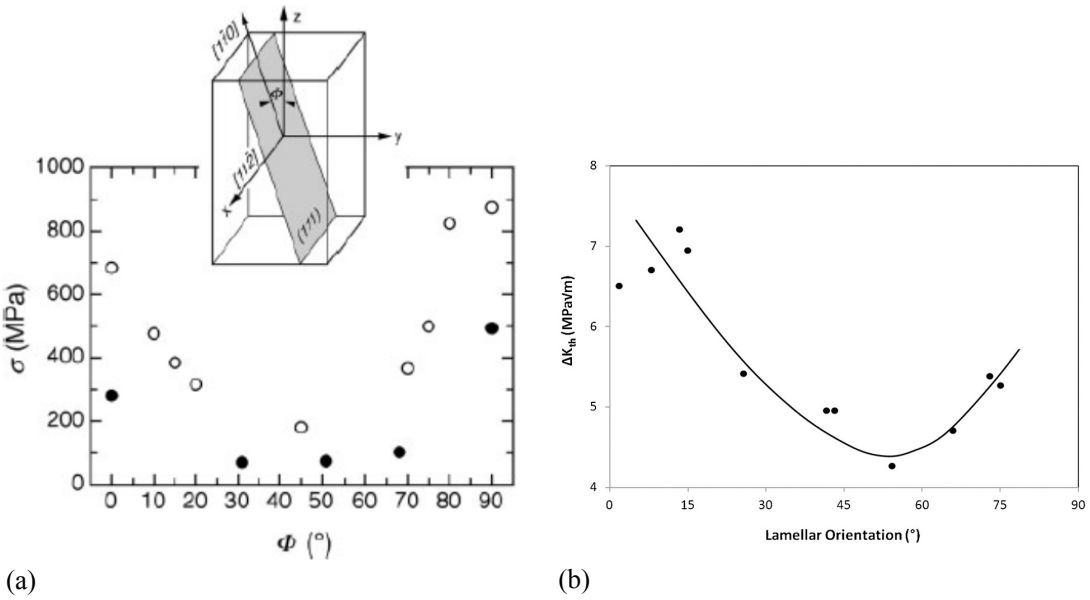

Figure 12. Yield stress of PST specimens as a function of the angle Φ at which the compression axis is inclined to the lamellar planes, from [8], using data from Fujiwara *et al.* [118] (black circles) and Nomura *et al.* [119] (white circles). (b) dependence of the fatigue threshold on the lamellar orientation, Φ, of the colony where the crack is propagating, from [117] (reproduced with permission). Note that both the yield stress and the fatigue threshold present a U-shaped curve against Φ, suggesting that there may be a same mechanistic cause to both.

45Al-2Mn-2Nb-1B as a function of both Φ and ΔK were determined. At ΔK values in the sub-/near-threshold range (< 10 MPa m$^{1/2}$), colonies with $0° < \Phi < 60°$ failed by translamellar fracture with relatively smooth fracture surfaces; only crack deviation along transverse slip bands and twins generated roughness. If instead the local ΔK was higher, secondary interlamellar cracking approximately parallel to the loading axis also occurred, resulting in increased roughness of the crack surfaces, which is generally recognised as beneficial towards reducing the effective ΔK by crack closure [9,17]. Hence the intrinsic cohesion of lamellar interfaces may be sufficient to resist interlamellar debonding as a secondary crack mechanism in the sub-/near-threshold regime. This lack of interlamellar cracking leaves the material without the benefits of crack closure in the threshold regime of crack growth for the $0° < \Phi < 60°$ orientations. Again, the secondary orientation, Ψ, was found to have no impact on the material fatigue properties. It should however be noted that fracture surfaces following gigacycle fatigue testing indicated that higher amounts of secondary cracking were generated in the testpieces loaded in excess of 10^7 cycles [31], and therefore at lower stresses, suggesting that a lower cycling stress applied for a more extended period can eventually generate secondary cracking.

The $\Phi \sim 90°$ orientation has generally been viewed as the weakest colony orientation [120]. In the study by Min *et al.* [62], the notched $\Phi \sim 90°$ colonies failed rapidly once cracking initiated (at consistently above 93% of the total life). This was followed by a much slower crack propagation in the lower Φ colonies beyond. This steady propagation regime beyond the $\Phi \sim 90°$ colony was identical to crack growth when cracking instead initiated in a colony with Φ closer to 0°. Debonding of the lamellar planes may be so easy that interlamellar cracking in $\Phi \sim 90°$ colonies ahead of the crack tip occurs, followed by crack expansion in the reverse direction, towards the crack tip, to sever bridging ligaments [78,112]. In contrast, Yang *et al.* [117] found the

$\Phi \sim 90°$ orientation to have an intermediate ΔK_{th}, between that of $\Phi \sim 0°$ (best) and $40° < \Phi < 65°$ (worst), Fig. 12(b). It may be that the issue of $\Phi \sim 90°$ colonies in [62] was overcome by the small colony size (70 µm, relative to 1 mm in [117]) such that the fatigue threshold was not exceeded after failure of a single $\Phi \sim 90°$ colony.

Another study [17] on a textured cast billet of Ti-48Al-2Cr-2Nb instead yielded no noticeable effect of Φ on ΔK_{th} or the Paris slope across a range of stress ratios, for loading at $\Phi = 0°$ and 90°. This may have been due to the testpieces not being sufficiently textured, whereby actual colony orientations varied within ∼40° of the nominal Φ.

5. Outlook for HCF research on TiAl alloys

5.1. Towards a microscopic model for HCF loading of TiAl alloys: a focus on plasticity

Within the field of TiAl alloy research, it is not clear what level of plasticity is optimal. Indeed, though there is a clear consensus that room temperature ductility should be raised, that is, increasing the elongation to failure, it is not clear how this influences the HCF life. This is not in the least because of conflicting interpretations of results, whereby almost identical electron images of interlamellar movement have been interpreted in different ways: micro-cracking [63,64,121], interlamellar sliding to form ledges [122] or longitudinal plasticity near the lamellar interface, see Fig. 13. Evidently, these mechanisms also have a varying degree of impact on fatigue crack formation and growth, as has been explored in section 3.

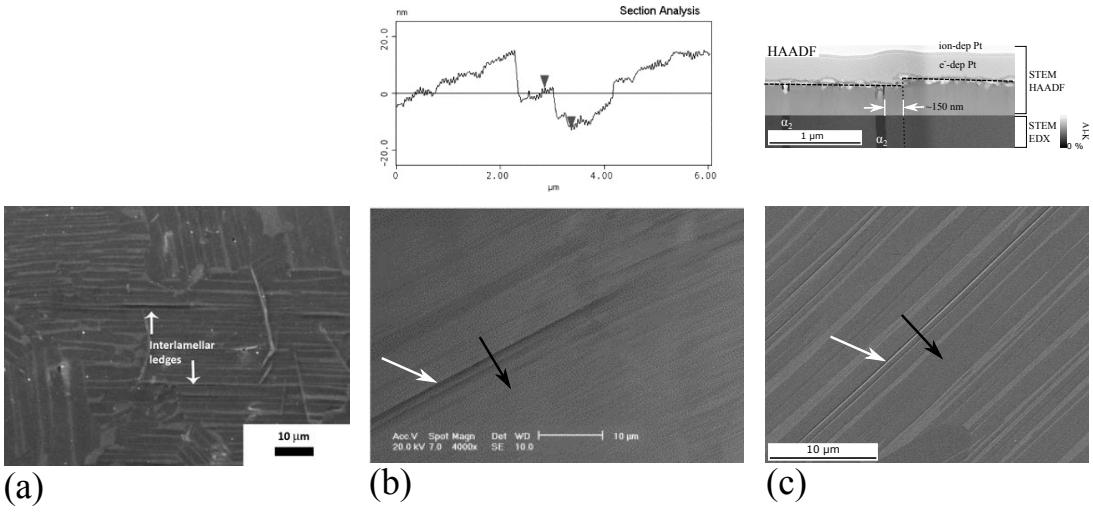

Figure 13. SEM images of similar deformation features near lamellar interfaces, interpreted as (a) ledges at lamellar interfaces [122], i.e. interfacial sliding, (b) interlamellar cracking [121], i.e. debonding of the lamellar interface, and (c) longitudinal slip in the γ-TiAl lamellae, near the lamellar interface [123]. Above (b): AFM linescan across the feature reported as interlamellar cracking; above (c): scanning transmission electron microscopy (STEM) images of a slip step near an α_2/γ interface. White arrows indicate the features of interest at the lamellar interfaces; black arrows are illustrative of AFM scan or cross-sectional imaging slice directions. (reproduced with permission).

The study of the HCF behaviour of γ-TiAl alloys has generally focused on plasticity in the region of a crack tip, rather than in the bulk of the material [65,105]. This is possibly because in common engineering alloys, achieving HCF loading to over 10^7

cycles often means operating at stresses considerably below the yield stress, so that to exceed the local critical resolved shear stress for slip, stress concentration at a crack tip, a hard particle or a crystal boundary is required. In contrast, due to the four-fold strength anisotropy of lamellar γ-TiAl alloys, Fig. 12(a), at $\sigma_{\max,\mathrm{th}}$ the softest colonies may be loaded well above their plastic limit for longitudinal slip and twin systems. So-called micro-plasticity may therefore occur throughout such colonies, regardless of the existence of other stress concentrators. Evidence for this is reviewed in the next section. Hence, the HCF cycling of lamellar γ-TiAl alloys may in fact involve a variety of deformation mechanisms, that vary from colony to colony, some of which are characteristic of LCF cycling (i.e. bulk plasticity), whilst other colonies do not deform plastically.

Current common procedure is to carry out fatigue crack growth testing of γ-TiAl alloys on stress relaxed, virgin material. Some data [64] has indicated that a single loading cycle below the general yield stress can have a significantly detrimental effect on the *S-N* behaviour of γ-TiAl alloys. In practice, a γ-TiAl component has to sustain HCF loading of an instantaneously imposed crack, as in the simulated object damage evoked in section 2.4, potentially towards the end of its lifecycle. Despite this, no representative investigations have been made of the effect of such extended HCF loading of initially uncracked material on the FCG behaviour once a pre-crack has been introduced. This might be achieved, for example, by loading a lamellar γ-TiAl alloy for 10^7 cycles at $\sigma_{\max,\mathrm{th}}$, then producing a FCG testpiece and performing a conventional FCG test to identify the effect on the fatigue threshold of this pre-conditioning of the material below the general yield stress.

Since the establishment of the continuous load shedding FCG measurement strategy standard ASTM E647 for crack threshold measurement [9,10], several further loading profiles have been proposed [124,125]. A range of the envisageable strategies is illustrated in Fig. 14. ASTM E647 corresponds to case (b); others in [124,125] are (g, i, j) and one of the non-standard ones (d) has been applied to a γ-TiAl alloy in [126]. In selecting a strategy for FCG testing of γ-TiAl, some of the considerations are as follows. Firstly, a constant $K_{\max}$ (right-hand column) facilitates separation of the p and q exponents in equation 2, where for intermetallics $p \sim q$. Depending on whether load is increased (c, g, k) or shed (a, e, i), the fatigue threshold is defined by the no-growth - growth transition, in either the forward or the reverse direction, respectively. This transition is defined in ASTM E647 to be at a growth rate of 10^{-10} m cycle^{-1}. Importantly, though, the size of the plastic zone ahead of the crack tip varies, being larger in decreasing ΔK loading than in increasing ΔK loading. In the loading strategies where a short loading period at a large stress intensity range, ΔK_0, precedes FCG testing, the fatigue crack must now grow in a very large plastic zone.

There is no consensus as to which test strategies are most damaging or conservative, as this may be material dependent. It is reported in other engineering alloys [125] that prior cycling, even below the no-growth limit, can significantly reduce the fatigue life: load-history can change the ranking of materials by FCG threshold. In a Ti-alloy, for example, the strategy (i) produced a lower value for the fatigue threshold than (g) [124], although (g) was thought to be more representative of conditions during practical use. Lerch *et al.* [127] have investigated the behaviour of a γ-TiAl alloy Ti-46.5Al-2Cr-2Nb upon step increases in the applied cyclic stress during tests aimed at determining the maximum run-out stress. No evidence of coaxing was found, that is to say that there is apparently no load history in this alloy resulting from strengthening by strain ageing at lower stress levels. This does not however preclude overstress cycles (even a single cycle) from having a significant impact on the fatigue life.

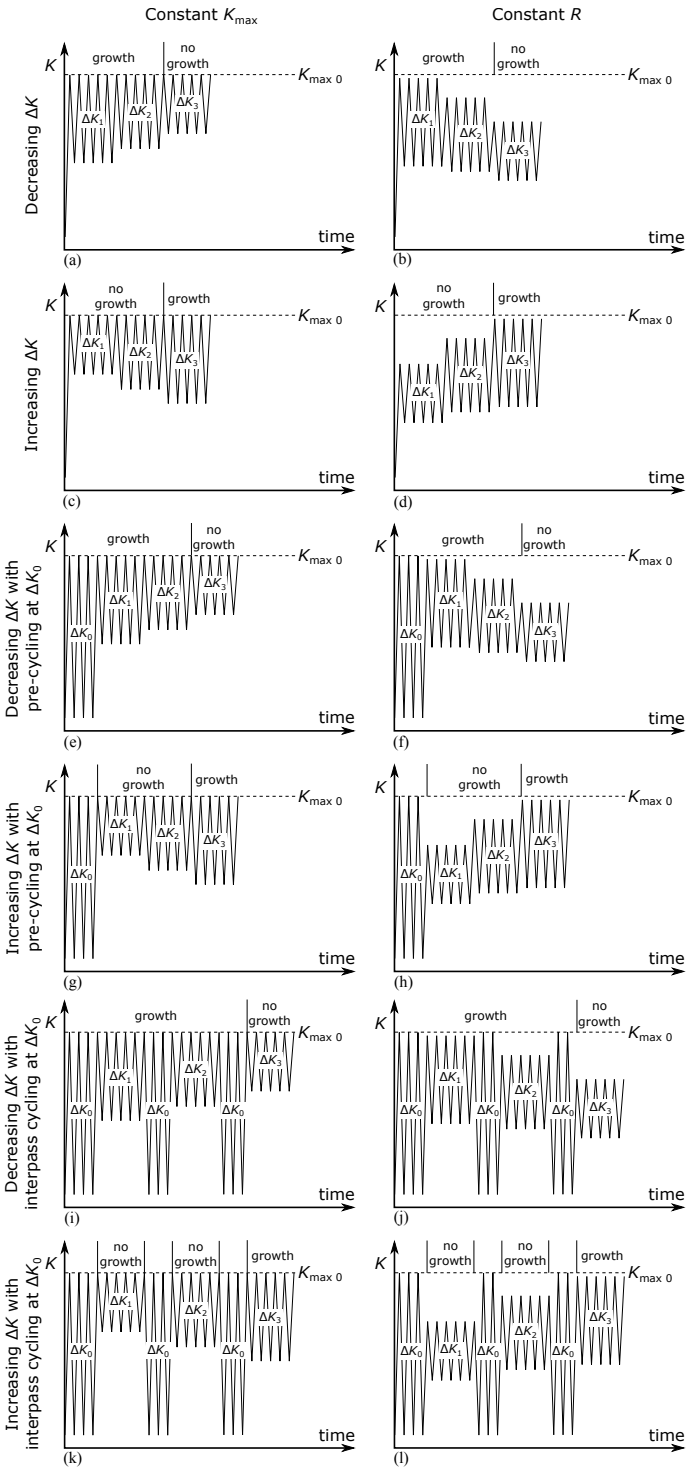

Figure 14. A selection of possible loading strategies for measuring the FCG rate da/dN as a function of ΔK, and hence determining the fatigue threshold where $da/dN = 10^{-10}$ m cycle^{-1} (growth/no-growth transition). The FCG specimen is loaded at ΔK_1 for an extended period (as per ASTM E647 [10]), followed by successive steps ΔK_2, ΔK_3, and so on, until a FCG rate of 10^{-10} m cycle^{-1} is either subceeded or exceeded, depending on whether ΔK is being decreased (a,b) or increased (c,d), respectively. Constant $K_{\max}$ and constant $R = K_{\min}/K_{\max}$ versions of each exist. Further, prior cycling at a large stress intensity range ΔK_0 for a short period (e - h) may serve to generate a large plastic zone ahead of the crack tip within which the near-threshold crack must then grow. Finally, the large ΔK_0 cycling may be applied between each step in ΔK_1, ΔK_2, ΔK_3 (i - l) to remove history effects of the previous loading step by forcing the near-threshold crack to grow in the same sized large plastic zone at each step. Extended from [124] (reproduced with permission).

For γ-TiAl alloys, although the shape of the crack tip plastic zone is known to be inconsistent with the predictions of continuum mechanics [105], the plastic zone size in application conditions is likely to be considerably different to that in a simple HCF test due to the additional underlying LCF or steady state loading to the component. This LCF can lead to both strengthening by work hardening, or microcracking [65], in the crack process zone. The above FCG testing strategies (i - l) are able to reproduce the salient features of the superimposed LCF and HCF loading, and may hence determine realistic or more conservative values for ΔK_{th}. A more systematic approach, by comparison of the effect of the different loading strategies in Fig. 14 on the measured fatigue thresholds, and an understanding of the underlying mechanistic reasons for this, may be necessary to gain confidence in the HCF lifing of γ-TiAl alloys.

Further, there has been little work on the variable amplitude fatigue properties of γ-TiAl alloys [22]. This is possibly surprising as HCF in the proposed applications results from the relaxation of vibrations [5], where the amplitude varies. In general, however, variable amplitude fatigue is a loading regime for which the theory is also not well understood [125].

5.2. Advances in understanding the distribution of strain in fatigue

Most of the studies on the fatigue of titanium aluminides where an effort has been made to seek a microstructural understanding of the deformation structures and mechanisms have used either scanning electron microscopy (SEM) to image flaw formation *in-situ* [59,62] or transmission electron microscopy (TEM) to image dislocation and twin structures in samples extracted after testing. However, an image of the dislocation structure at one instance does not allow the plastic strain accumulated thus far in that region to be determined. Even techniques such as high-resolution electron backscatter diffraction (HR-EBSD) [128], do not capture this as they measure only the elastic strain and rotation of the lattice, rather than the permanent, plastic strain associated with dislocation motion.

Work by Beran *et al.* [129], has enabled post-mortem TEM observations to be confirmed by *in situ* neutron diffraction during the cyclic loading of the testpiece. The volume fraction of deformation twins in the γ-TiAl phase was hence measured by both techniques; it rarely exceeded 0.025. Twinning as a plasticity mechanism in fatigue was found to be rapidly exhausted.

The past two decades has seen substantial progress in the field of digital image correlation (DIC) strain mapping [130], whereby the strain tensor for deformation in the surface plane is obtained by matching the positions of fiducial surface features before and after deformation. The strain developed between individual areas only 44×44 nm^2 [131] in size can be measured by imaging in an SEM. Similarly to HR-EBSD, this technique is non-destructive and hence may be applied throughout the fatigue cycling of a testpiece. The first application of DIC strain mapping to TiAl alloys was made by Jiang *et al.* [132] on Ti-44Al-8Nb-1B loaded monotonically at room temperature in tension to just below and above the yield stress to characterise microplasticity. Elsewhere, Niendorf *et al.* [133] cyclically loaded Ti-45Al-5Nb-0.2B-0.2C (TNB-V5) at 25 °C and 700 °C to successively higher loads until failure, with regular pauses at maximum load to image the surface for DIC strain mapping. Niendorf *et al.* demonstrated that the origin of final fracture within the gauge length upon LCF loading could be determined by DIC strain mapping after only 20% of the total fatigue life. Jiang *et al.* were able to show that in lamellar and nearly lamellar microstructures, plasticity first occurs

at only ∼75% of the 0.2% proof stress, although in duplex microstructures this early onset was not seen; this was supported by post-mortem TEM imaging. However, both studies suffered from insufficient resolution in the strain maps to determine the exact location and distribution of plasticity relative to the lamellar microstructures. This was mainly due to their use of optical microscopy for image acquisition and insufficiently refined surface speckle patterns for higher resolution mapping.

More recent and extensive use of the DIC technique on TiAl alloys has been made by Filippini and co-workers [46,134–136]. They have measured the accumulation of plastic strain during monotonic and LCF loading of Ti-48Al-2Cr-2Nb testpieces with a duplex microstructure. Despite optical microscopy also being employed for pattern imaging, sufficient resolution was achieved to measure some local variations in the distribution of plastic strain between successive α_2-Ti_3Al and γ-TiAl lamellae, and the effect of lamellar orientation to the loading axis. Strain accumulation was identified in the vicinity of α_2/γ lamellar interfaces in soft-mode oriented lamellar colonies, see Fig. 15. This was consistent with DIC results obtained by Bode *et al.* [42] on an alloy of composition Ti-46.5Al-2.5V-1Cr. In both cases, lamellar orientations to the loading axis were obtained from measurement of surface traces. However, soft mode colonies might present a surface trace perpendicular to the loading axis and thereby appear to be hard mode colonies, and vice-versa. Attempts were made to assess the error in this by resolving strains along lamellae to calculate a minimum bound of confidence for the local plastic shear strain [134].

All DIC studies thus far on γ-TiAl alloys have used etching or sand blasting to produce the speckle pattern. To date, no systematic assessment exists of the effects of etching on the surface strains measured by DIC. However, these patterning methods may have preferentially weakened the lamellar interfaces and the colony boundaries and thereby caused strain to accumulate in these regions more so than on a flat, polished surface.

In short, digital image correlation strain mapping can measure the accumulation of local plasticity and damage during cyclic loading of γ-TiAl alloys. If applied using a high temperature stable nano-scale overlay speckle pattern [137,138], combined with SEM imaging [139,140], it has the opportunity to map plastic flow to the scale of individual γ lamellar domains, at aero-engine operational temperatures, without artificially weakening microstructural features. This would enable the location of slip/twin deformation during HCF, as well as crack initiation, to be studied as already achieved in other metallurgical systems [141].

5.3. A remark about alloy compositions

The present review has not focused on alloy compositions. One may note, as in [5], that conventional Ti alloy development has seen many incremental improvements in composition, and hence successive material replacements, without much change to processing. In contrast, for γ-TiAl alloys, most of the currently preferred and applied chemistries were developed over 20 years ago, e.g. Ti-48Al-2Cr-2Nb. The development of alloy compositions targeted at improving the strength and reliability of TiAl alloys under HCF loading at operational temperatures is being hindered by a lack of clarity as to optimal microstructures. Recognising that microstructural parameters and strengthening mechanisms beneficial to single colony (PST) components are not necessarily optimal for polycrystalline structures, and vice-versa, might facilitate more directed compositional development.

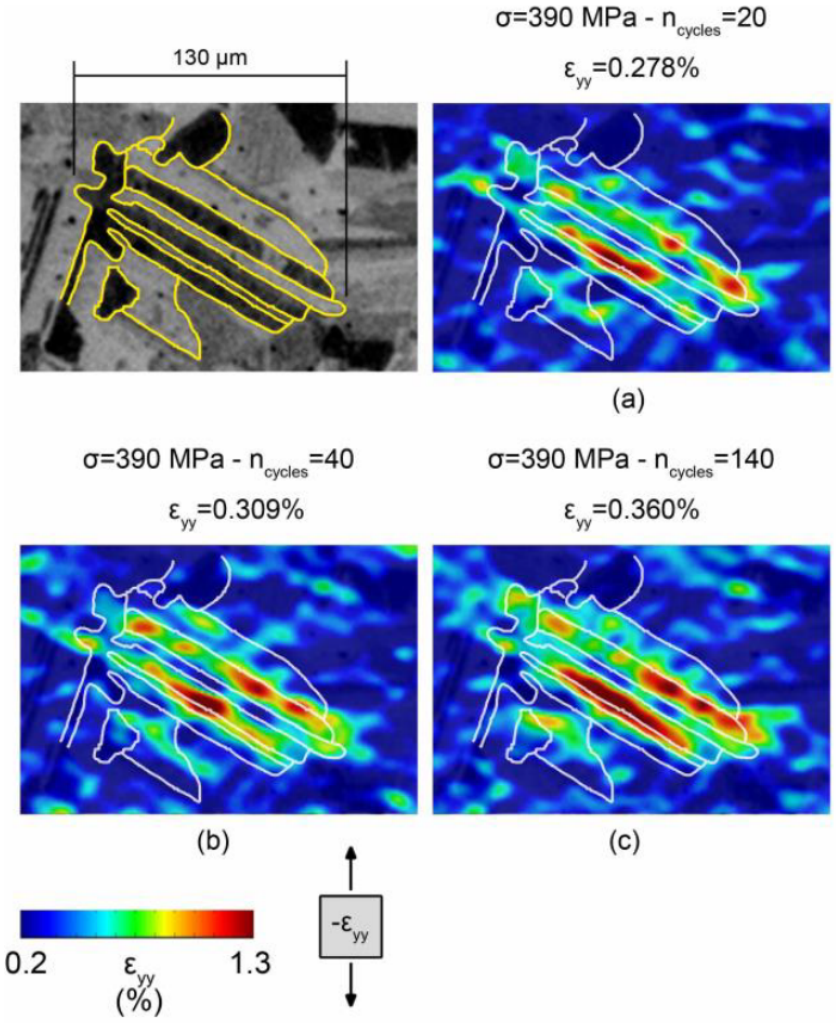

Figure 15. High resolution digital image correlation strain map for a lamellar grain captured from a sample cyclically loaded (*ex-situ*) in compression at a maximum nominal stress of 390 MPa and $R = 0.05$. Strain accumulates inside the defined lamellar platelets which are composed by the γ-TiAl phase. From [135] (reproduced with permission).

An example of how the composition might be tailored for improved HCF properties is to consider secondary cracking by interlamellar debonding, which is a potential toughening mechanism that might be exploited in colonies where translamellar cracking prevails, e.g. in $\Phi = 0°$ PST and columnar grained components. It was mentioned in section 4.3 that this mechanism does not operate in Ti-45Al-2Mn-2Nb-1B at stress intensity factors close to the threshold value, yet it is in this regime that TiAl alloys are to be operated. Furthermore, in untextured polycrystalline alloys, interlamellar debonding in $\Phi \sim 90°$ colonies can lead to crack initiation; absorption of mechanical energy by interlamellar debonding is therefore undesirable in such microstructures. Measurements of the lamellar cohesion energy, its dependence on Al content and other alloying elements, and an understanding of the mechanisms therefor, are scarce. Difficulty arises because accurate compositional measurements with lamellar scale resolution, e.g. by STEM-EDX [142], are difficult given the light elements present (Al, C, B) [143]. On the other hand, atom probe tomography (APT) studies of lamellar TiAl [144–147] have the potential to quantify the partitioning of elements to interfaces [148]. The accumulation of C in Ti-43Al-4Nb-1Mo-0.1B-0.75C (TNM) at a β_0/γ interface was recently measured [146,149], Fig. 16. The lamellar cohesion strength also depends on the composition of the matrix, which defines the local stresses associated with semi-coherency at the interface. Direct microscale measurement of the interfacial strength is possible [150], however current methods can generate spurious results, stemming from the sample preparation process [151]. Density functional theory modelling of interfacial energies for differing γ/γ interface types exists [152], however a more systematic analysis of the effect of a range of alloying elements on the interlamellar misfit stresses is lacking. In short, if γ-TiAl alloy compositions are to be tailored for HCF performance, an improved understanding of how solutes influence the interlamellar cohesion strength would be beneficial, and is achievable with current methods.

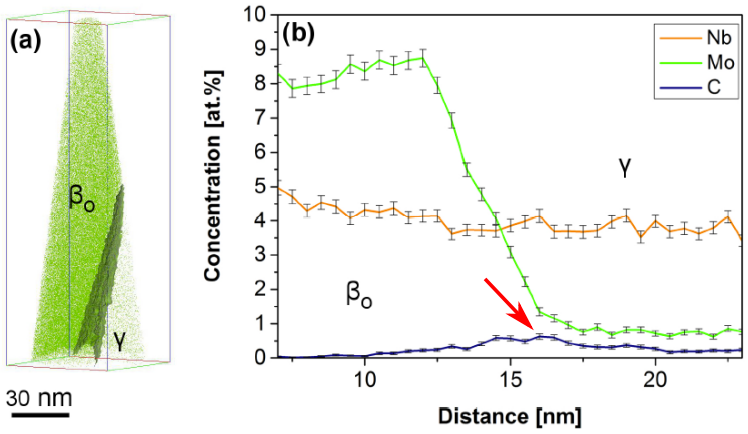

Figure 16. Atom probe tomography reconstruction of the β_0/γ interface in Ti-43Al-4Nb-1Mo-0.1B-0.75C. Note the peak in C, arrowed in red, near the interface; variations in the C content at the interface may change the cohesion strength of the β_0/γ interface. Adapted from [146] (reproduced with permission).

6. Summary

A summary of the conclusions drawn from the present review with regards to improving the lamellar γ-TiAl microstructure for HCF, depending on the morphology and

orientation of the lamellar colonies, is given in Table 2.

Microstructure	Polysynthetically twinned			Directionally solidified (columnar)			Polycrystalline
Φ	0°	45°	90°	0°	45°	90°	atextured
Optimal lamellar orientation	+			+			N/A
Optimal colony size		N/A			unknown		50 - 100 µm
Optimal lamellar thickness				refined (< 1 µm, at least)			
Plasticity (mainly longitudinal)	+	-	+	+	-	+	unknown
Interlamellar debonding	+	+	-	+	+	-	-

Table 2. Summary of the microstructural properties to optimise for improved HCF behaviour of fully or nearly lamellar γ-TiAl alloys as a function of lamellar orientation, Φ. +: mechanism to be promoted; -: mechanism to be inhibited or avoided.

Acknowledgement

Prof. W. J. Clegg is greatly thanked for fruitful discussions and proof reading this manuscript. The work was supported by the EPSRC / Rolls-Royce Strategic Partnership (EP/M005607/1). T.E.J.E. also acknowledges the kind support of the Worshipful Company of Armourers and Brasiers Gauntlet Trust.

References

[1] B. P. Bewlay, S. Nag, A. Suzuki, and M. J. Weimer, "TiAl alloys in commercial aircraft engines," *Materials at High Temperatures*, vol. 33, no. 4-5, pp. 549–559, 2016.

[2] I. Goold, "Rolls-Royce advances toward ultrafan," report, 2014.

[3] T. Tetsui and Y. Miura, "Heat-resistant cast TiAl alloy for passenger vehicle turbochargers," *Technical Review, Mitsubishi Heavy Industries, Ltd*, vol. 39, no. 1, pp. 1–5, 2002.

[4] H. Zhu, T. Wei, D. Carr, R. Harrison, L. Edwards, W. Hoffelner, D. Seo, and K. Maruyama, "Assessment of titanium aluminide alloys for high-temperature nuclear structural applications," *Journal of the Minerals, Metals, and Materials Society*, vol. 64, no. 12, pp. 1418–1424, 2012.

[5] D. Rugg, M. Dixon, and J. Burrows, "High-temperature application of titanium alloys in gas turbines. material life cycle opportunities and threats an industrial perspective," *Materials at High Temperatures*, vol. 33, no. 4-5, pp. 536–541, 2016.

[6] W. Smarsly, J. Esslinger, and H. Clemens, "Status of titanium aluminide for aero engine applications," in *IWTA2016*, 2016.

[7] G. Hénaff and A.-L. Gloanec, "Fatigue properties of TiAl alloys," *Intermetallics*, vol. 13, no. 5, pp. 543–558, 2005.

[8] F. Appel, J. D. H. Paul, and M. Oehring, *Gamma titanium aluminide alloys : science and technology*. Weinheim: Wiley-VCH, 2011.

[9] S. Suresh, *Fatigue of Materials*. Cambridge University Press, 1998.

[10] "Standard test method for measurement of fatigue crack growth rates," standard, ASTM International, West Conshohocken, PA, USA, 2015.

[11] P. Paris and F. Erdogan, "A critical analysis of crack propagation laws," *Journal of Basic Engineering*, vol. 85, no. 4, pp. 528–533, 1963.

[12] J. J. Kruzic, J. P. Campbell, A. L. McKelvey, H. Choe, and R. O. Ritchie in *Gamma Titanium Aluminides 1999* (Y.-W. Kim, D. M. Dimiduk, and M. H. Loretto, eds.), TMS, 1999.

[13] R. O. Ritchie and R. H. Dauskardt, "Cyclic fatigue of ceramics," *Journal of the Ceramic Society of Japan*, vol. 99, no. 1154, pp. 1047–1062, 1991.

[14] M. Hojo, K. Tanaka, C. G. Gustafson, and R. Hayashi, "Effect of stress ratio on near-threshold propagation of delimination fatigue cracks in unidirectional CFRP," *Composites Science and Technology*, vol. 29, no. 4, pp. 273–292, 1987.

[15] R. O. Ritchie, C. J. Gilbert, and J. M. McNaney, "Mechanics and mechanisms of fatigue damage and crack growth in advanced materials," *International Journal of Solids and Structures*, vol. 37, no. 1, pp. 311–329, 2000.

[16] M. Filippini, S. Beretta, L. Patriarca, G. Pasquero, and S. Sabbadini, "Fatigue sensitivity to small defects of a gamma-titanium aluminide alloy," *Journal of ASTM International*, vol. 9, no. 5, pp. 1–12, 2012.

[17] M. S. Dahar, S. M. Seifi, B. P. Bewlay, and J. J. Lewandowski, "Effects of test orientation on fracture and fatigue crack growth behavior of third generation as-cast Ti48Al2Nb2Cr," *Intermetallics*, vol. 57, no. 0, pp. 73–82, 2015.

[18] C. Mabru, D. Bertheau, S. Pautrot, J. Petit, and G. Hénaff, "Influence of temperature and environment on fatigue crack propagation in a TiAl-based alloy," *Engineering Fracture Mechanics*, vol. 64, no. 1, pp. 23–47, 1999.

[19] R. C. Feng, Z. Y. Rui, Y. Zuo, C. F. Yan, and G. T. Zhang, "Influence of temperature on fatigue crack propagation in TiAl alloys," *Strength of Materials*, vol. 46, no. 3, pp. 417–421, 2014.

[20] P. Bowen, R. A. Chave, and A. W. James, "Cyclic crack growth in titanium aluminides," *Materials Science and Engineering: A*, vol. 192-193, pp. 443 – 456, 1995. 3rd International Conference on High Temperature Intermetallics.

[21] G. Chen, Y. Peng, G. Zheng, Z. Qi, M. Wang, H. Yu, C. Dong, and C. T. Liu, "Polysynthetic twinned TiAl single crystals for high-temperature applications," *Nature Materials*, vol. 15, no. 8, pp. 876–881, 2016.

[22] A. L. Gloanec, G. Hénaff, D. Bertheau, P. Belaygue, and M. Grange, "Fatigue crack growth behaviour of a gamma-titanium-aluminide alloy prepared by casting and powder metallurgy," *Scripta Materialia*, vol. 49, no. 9, pp. 825–830, 2003.

[23] Y. R. Zuo, Z. Y. Rui, R. C. Feng, D. C. Luo, and C. F. Yan, "Influence of microstructure and stress ratio on fatigue crack propagation in TiAl alloy," *Advanced Materials Research*, vol. 881, pp. 1330–1333, 2014.

[24] L. E. Andersson and M. Larsson, "Device and arrangement for producing a three-dimensional object," 2005. EP Patent 1,296,788.

[25] S. Biamino, A. Penna, U. Ackelid, S. Sabbadini, O. Tassa, P. Fino, M. Pavese, P. Gennaro, and C. Badini, "Electron beam melting of Ti48Al2Cr2Nb alloy: Microstructure and mechanical properties investigation," *Intermetallics*, vol. 19, no. 6, pp. 776–781, 2011.

[26] J. M. Larsen, A. H. Rosenberger, B. D. Worth, K. Li, D. C. Maxwell, and W. J. Porter, "Assuring reliability of gamma titanium aluminides in long-term service," *Minerals, Metals and Materials Society/AIME, Gamma Titanium Aluminides 1999(USA)*, pp. 463–472, 1999.

[27] Y. Zhou, J. Q. Wang, B. Zhang, W. Ke, and E. H. Han, "High-temperature fatigue property of Ti46Al8Nb alloy with the fully lamellar microstructure," *Intermetallics*, vol. 24, pp. 7–14, 2012.

[28] H. Q. Xue, H. Tao, F. Montembault, Q. Y. Wang, and C. Bathias, "Development of a three-point bending fatigue testing methodology at 20 kHz frequency," *International Journal of Fatigue*, vol. 29, no. 911, pp. 2085–2093, 2007.

[29] C. Bathias, *Fatigue of materials and structures*. John Wiley & Sons, 2013.

[30] H. Xue, H. Tao, E. Bayraktar, and C. Bathias, "High-cycle fatigue of a TiAl alloy in three-point bending test," *Jixie Qiangdu/Journal of Mechanical Strength*, vol. 30, no. 1, pp. 112–116, 2008.

[31] E. Bayraktar, C. Bathias, X. Hongquian, and T. Hao, "On the giga cycle fatigue behaviour of two-phase ($\alpha 2+\gamma$) TiAl alloy," *International Journal of Fatigue*, vol. 26, no. 12, pp. 1263–1275, 2004.
[32] W. Elber, *The significance of fatigue crack closure.* ASTM International, 1971.
[33] G. R. Halford, *Fatigue and durability of structural materials.* ASM International, 2006.
[34] R. A. Schmidt and P. C. Paris, *Threshold for fatigue crack propagation and the effects of load ratio and frequency.* ASTM International, 1973.
[35] G. Hénaff, S.-A. Cohen, C. Mabru, and J. Petit, "The role of crack closure in fatigue crack propagation behaviour of a TiAl-based alloy," *Scripta Materialia*, vol. 34, no. 9, pp. 1449–1454, 1996.
[36] B. D. Worth, J. M. Larsen, S. J. Balsone, and J. W. Jones, "Mechanisms of ambient temperature fatigue crack growth in Ti-46.5Al-3Nb-2Cr-0.2W," *Metallurgical and Materials Transactions A*, vol. 28, no. 13, pp. 825–835, 1997.
[37] W. O. Soboyejo, J. E. Deffeyes, and P. B. Aswath, "Investigation of room- and elevated-temperature fatigue crack growth in Ti-48Al," *Materials Science and Engineering: A*, vol. 138, no. 1, pp. 95–101, 1991.
[38] A. L. McKelvey, K. T. V. Rao, and R. O. Ritchie, "On the anomalous temperature dependence of fatigue-crack growth in γ-based titanium aluminides," *Scripta Materialia*, vol. 37, no. 11, pp. 1797–1803, 1997.
[39] J. P. Campbell, J. J. Kruzic, S. Lillibridge, K. T. V. Rao, and R. O. Ritchie, "On the growth of small fatigue cracks in γ-based titanium aluminides," *Scripta Materialia*, vol. 37, no. 5, pp. 707–712, 1997.
[40] J. J. Kruzic, J. P. Campbell, and R. O. Ritchie, "On the fatigue behavior of γ-based titanium aluminides: role of small cracks," *Acta Materialia*, vol. 47, no. 3, pp. 801–816, 1999.
[41] K. S. Chan and D. S. Shih, "Fatigue and fracture behavior of a fine-grained lamellar TiAl alloy," *Metallurgical and Materials Transactions A*, vol. 28, no. 1, pp. 79–90, 1997.
[42] B. Bode, W. Wessel, A. Brueckner-Foit, J. Mildner, M. Wollenhaupt, and T. Baumert, "Local deformation at micro-notches and crack initiation in an intermetallic γ-TiAl-alloy," *Fatigue & Fracture of Engineering Materials & Structures*, vol. 39, no. 2, pp. 227–237, 2016.
[43] W. Wessel, *Mikrostrukturelle Untersuchungen der Rissinitiierung und -ausbreitung in intermetallischen TiAl-Legierungen unter zyklischer und quasistatischer Belastung.* PhD thesis, 2012.
[44] W. Wessel, J. Mildner, P. Pitz, A. Brueckner-Foit, M. Wollenhaupt, and T. Baumert, "Micronotches for studying growth of small cracks," *Fatigue & Fracture of Engineering Materials & Structures*, vol. 38, no. 6, pp. 673–680, 2015.
[45] W. Wessel, F. Zeismann, and A. Brueckner-Foit, "Short fatigue cracks in intermetallic γ-TiAl-alloys," *Fatigue & Fracture of Engineering Materials & Structures*, vol. 38, no. 12, pp. 1507–1518, 2015.
[46] M. Filippini, S. Beretta, L. Patriarca, and S. Sabbadini, "Effect of the microstructure on the deformation and fatigue damage in a gamma-TiAl produced by additive manufacturing," in *Gamma Titanium Aluminide Alloys 2014*, pp. 189–193, John Wiley & Sons, Inc., 2014.
[47] K. Tanaka, Y. Nakai, and M. Yamashita, "Fatigue growth threshold of small cracks," *International Journal of Fracture*, vol. 17, no. 5, pp. 519–533, 1981.
[48] T. S. Harding and J. Wayne Jones, "The effect of impact damage on the room-temperature fatigue behavior of γ-TiAl," *Metallurgical and Materials Transactions A*, vol. 31, no. 7, pp. 1741–1752, 2000.
[49] S. L. Draper, M. V. Nathal, B. A. Lerch, J. M. Pereira, C. M. Austin, and O. Erdmann, "The effect of ballistic impacts on the high-cycle fatigue properties of Ti-48Al-2Nb-2Cr (atomic percent)," *Metallurgical and Materials Transactions A*, vol. 32, no. 11, pp. 2743–2758, 2001.
[50] S. L. Draper, B. A. Lerch, J. M. Pereira, M. V. Nathal, M. Nazmy, M. Staubli, and D. R.

Clemens, "Effect of impact damage on the fatigue response of TiAl alloy - ABB-2," in *Stuctural intermetallics* (K. J. Hemker, ed.), pp. 295–304, The Minerals, Metals and Materials Society.

[51] P. S. Stief, M. P. Rubal, G. T. Gray Iii, and J. M. Pereiras, "Damage in gamma titanium aluminides due to small particle impacts," *Journal of the Mechanics and Physics of Solids*, vol. 46, no. 10, pp. 2069–2086, 1998.

[52] S. L. Draper and B. A. Lerch, "Durability assessment of TiAl alloys," in *Gamma Titanium Aluminides 2008*, The Minerals, Metals and Materials Society.

[53] M. R. Bache and C. C. Morgans, "Domestic object damage and fatigue behaviour of an advanced gamma TiAl alloy," *Intermetallics*, vol. 19, no. 6, pp. 782–786, 2011.

[54] T. Kruml, K. Obrtlík, M. Petrenec, and J. Polák, "Cyclic response and fatigue life of TiAl alloys at high temperatures," *Key Engineering Materials*, vol. 417-418, pp. 585–588, 2010.

[55] M. Petrenec, P. Buek, T. Kruml, and J. Polák, "Effect of temperature on the cyclic stress components of gamma - TiAl based alloy with niobium alloying," *Key Engineering Materials*, vol. 465, pp. 447–450, 2011.

[56] A. Chlupová, K. Obrtlík, P. Beran, M. Heczko, J. Polák, and T. Kruml, "Monotonic and cyclic properties of TiAl alloys doped with Nb, Mo and C," *Procedia Engineering*, vol. 74, pp. 405–408, 2014.

[57] T. Kruml, A. Chlupová, and K. Obrtlík, "Cyclic deformation of a modern TiAl alloy at high temperatures," *Advanced Materials Research*, vol. 891-892, pp. 1131–1136, 2014.

[58] T. Kruml and K. Obrtlík, "Microstructure degradation in high temperature fatigue of TiAl alloy," *International Journal of Fatigue*, vol. 65, pp. 28–32, 2014.

[59] L. Yu, X. Song, M. Zhang, Z. Jiao, and H. Yu, "Effect of stress ratio on fatigue lifetime of high Nb containing TiAl alloy at elevated temperature," *Materials & Design*, vol. 84, pp. 378–384, 2015.

[60] A. H. Rosenberger, B. D. Worth, J. M. Larsen, M. V. Nathal, R. Darolia, C. T. Liu, P. L. Martin, D. B. Miracle, R. Wagner, and M. Yamaguchi in *Structural Intermetallics 1997*, p. 555, TMS, Warrendale, PA, USA, 1997.

[61] G. Hénaff, G. Odemer, and A. Tonneau-Morel, "Environmentally-assisted fatigue crack growth mechanisms in advanced materials for aerospace applications," *International Journal of Fatigue*, vol. 29, no. 911, pp. 1927–1940, 2007.

[62] Z. Min, S. Xi-ping, Y. Long, L. Hong-liang, J. Ze-hui, and Y. Hui-chen, "In situ observation of fatigue crack initiation and propagation behavior of a high-Nb TiAl alloy at 750 C," *Materials Science and Engineering: A*, vol. 622, pp. 30–36, 2015.

[63] R. Botten, X. Wu, D. Hu, and M. H. Loretto, "The significance of acoustic emission during stressing of TiAl-based alloys. Part I: Detection of cracking during loading up in tension," *Acta Materialia*, vol. 49, no. 10, pp. 1687–1691, 2001.

[64] X. Wu, D. Hu, R. Botten, and M. H. Loretto, "The significance of acoustic emission during stressing of TiAl-based alloys. Part II: Influence of cracks induced by pre-stressing on the fatigue life," *Acta Materialia*, vol. 49, no. 10, pp. 1693–1699, 2001.

[65] B. C. Ng, B. A. Simkin, M. A. Crimp, and T. R. Bieler, "The role of mechanical twinning on microcrack nucleation and crack propagation in a near-γ TiAl alloy," *Intermetallics*, vol. 12, no. 12, pp. 1317–1323, 2004.

[66] S. K. Jha, J. M. Larsen, and A. H. Rosenberger, "The role of competing mechanisms in the fatigue life variability of a nearly fully-lamellar γ-TiAl based alloy," *Acta Materialia*, vol. 53, no. 5, pp. 1293–1304, 2005.

[67] B. Han, W. J. Wan, C. L. Zhu, J. Zhang, and J. H. Yi, "Effect of casting defects on high cycle fatigue life of fully lamellar TiAl alloy," *Materials Research Innovations*, vol. 19, no. sup4, pp. S142–S146, 2015.

[68] W. Weibull, "A statistical theory of strength of materials," in *Proceedings of the Royal Swedish Institute, Engineering Research No. 151*, 1939.

[69] Y. Umakoshi, H. Y. Yasuda, and T. Nakano, "Plastic anisotropy and fatigue of TiAl PST crystals: a review," *Intermetallics*, vol. 4, Supplement 1, pp. S65–S75, 1996.

[70] R. Lebensohn, H. Uhlenhut, C. Hartig, and H. Mecking, "Plastic flow of γ-TiAl-based polysynthetically twinned crystals: micromechanical modeling and experimental validation," *Acta Materialia*, vol. 46, no. 13, pp. 4701–4709, 1998.
[71] B. K. Kad and R. J. Asaro, "Apparent Hall-Petch effects in polycrystalline lamellar TiAl," *Philosophical Magazine A*, vol. 75, no. 1, pp. 87–104, 1997.
[72] B. A. Simkin, B. C. Ng, M. A. Crimp, and T. R. Bieler, "Crack opening due to deformation twin shear at grain boundaries in near-γ TiAl," *Intermetallics*, vol. 15, no. 1, pp. 55–60, 2007.
[73] T. E. J. Edwards, F. Di Gioacchino, R. Muñoz-Moreno, and W. J. Clegg, "The interaction of borides and longitudinal twinning in polycrystalline TiAl alloys," *Acta Materialia*, vol. 140, no. Supplement C, pp. 305–316, 2017.
[74] Y. H. Lu, Y. G. Zhang, L. J. Qiao, Y. B. Wang, C. Q. Chen, and W. Y. Chu, "In-situ TEM study of fracture mechanisms of polysynthetically twinned (PST) crystals of TiAl alloys," *Materials Science and Engineering: A*, vol. 289, no. 1, pp. 91–98, 2000.
[75] A. H. Cottrell, "Theory of brittle fracture in steel and similar metals," *Transactions of the Metallurgical Society AIME*, vol. 212, 1958.
[76] Z. W. Huang and P. Bowen, "Persistent microslip bands in the lamellar TiAl structure subjected to room temperature fatigue," *Scripta Materialia*, vol. 45, no. 8, pp. 931–937, 2001.
[77] R. Ding, H. Li, D. Hu, N. Martin, M. Dixon, and P. Bowen, "Features of fracture surface in a fully lamellar TiAl-base alloy," *Intermetallics*, vol. 58, pp. 36–42, 2015.
[78] J. Yang, H. Li, D. Hu, and M. Dixon, "Microstructural characterisation of fatigue crack growth fracture surfaces of lamellar Ti45Al2Mn2Nb1B," *Intermetallics*, vol. 45, no. 0, pp. 89–95, 2014.
[79] M. Filippini, S. Beretta, L. Patriarca, G. Pasquero, and S. Sabbadini, "Defect tolerance of a gamma titanium aluminide alloy," *Procedia Engineering*, vol. 10, pp. 3677–3682, 2011.
[80] T. Leitner, M. Schloffer, S. Mayer, J. Elinger, H. Clemens, and R. Pippan, "Fracture and R-curve behavior of an intermetallic β-stabilized TiAl alloy with different nearly lamellar microstructures," *Intermetallics*, vol. 53, pp. 1–9, 2014.
[81] Z.-J. Yang, H.-L. Sun, Z.-W. Huang, X.-S. Jiang, and S. Chen, "Fatigue properties of a medium-strength γ-TiAl alloy with different surface conditions," *Rare Metals*, vol. 35, no. 1, pp. 93–99, 2016.
[82] J. P. Campbell, R. O. Ritchie, and K. T. Venkateswara Rao, "The effect of microstructure on fracture toughness and fatigue crack growth behavior in γ-titanium aluminide based intermetallics," *Metallurgical and Materials Transactions A*, vol. 30, no. 3, pp. 563–577, 1999.
[83] R. O. Ritchie and S. Suresh, "Some considerations on fatigue crack closure at near-threshold stress intensities due to fracture surface morphology," *Metallurgical Transactions A*, vol. 13, no. 5, pp. 937–940, 1982.
[84] M. Filippini, M. Schloffer, E. Crist, R. Haun, A. Muth, T. Edwards, M. S. Dahar, D. M. Dimiduk, and Y.-W. Kim, "Panel discussion: microstructure-defects-life," in *GAT2017 at TMS 2017*, 2017.
[85] H. Clemens and S. Mayer, "Design, processing, microstructure, properties, and applications of advanced intermetallic TiAl alloys," *Advanced Engineering Materials*, vol. 15, no. 4, pp. 191–215, 2013.
[86] D. M. Dimiduk, P. M. Hazzledine, T. A. Parthasarathy, M. G. Mendiratta, and S. Seshagiri, "The role of grain size and selected microstructural parameters in strengthening fully lamellar TiAl alloys," *Metallurgical and Materials Transactions A*, vol. 29, no. 1, pp. 37–47, 1998.
[87] Y.-W. Kim, "Effects of microstructure on the deformation and fracture of γ-TiAl alloys," *Materials Science and Engineering: A*, vol. 192193, Part 2, no. 0, pp. 519–533, 1995.
[88] K. S. Chan and Y.-W. Kim, "Influence of microstructure on crack-tip micromechanics and fracture behaviors of a two-phase TiAl alloy," *Metallurgical Transactions A*, vol. 23,

no. 6, pp. 1663–1677, 1992.
[89] N. J. Rogers, P. D. Crofts, I. P. Jones, and P. Bowen, "Microstructure toughness relationships in fully lamellar γ-based titanium aluminides," *Materials Science and Engineering: A*, vol. 192, pp. 379–386, 1995.
[90] G. Cao, L. Fu, J. Lin, Y. Zhang, and C. Chen, "The relationships of microstructure and properties of a fully lamellar TiAl alloy," *Intermetallics*, vol. 8, no. 56, pp. 647–653, 2000.
[91] Y. Mine, K. Takashima, and P. Bowen, "Effect of lamellar spacing on fatigue crack growth behaviour of a TiAl-based aluminide with lamellar microstructure," *Materials Science and Engineering: A*, vol. 532, pp. 13–20, 2012.
[92] D. Lin and M. Chen, "Interaction between deformation process and lamellar interfaces in polysynthetically twinned (PST) crystals of TiAl," in *Gamma titanium aluminides 1995*, pp. 323–330, Minerals, Metals and Materials Society, Warrendale, PA, US, 1995.
[93] Y. Umakoshi, H. Y. Yasuda, and T. Nakano, "Plastic anisotropy and fracture behavior of cyclically deformed TiAl polysynthetically twinned crystals," *Materials Science and Engineering: A*, vol. 192, pp. 511–517, 1995.
[94] Y. Umakoshi and T. Nakano, "Plastic behaviour of TiAl crystals containing a single set of lamellae at high temperatures," *ISIJ international*, vol. 32, no. 12, pp. 1339–1347, 1992.
[95] Z. W. Huang and W. Hu, "Thermal stability of an intermediate strength fully lamellar Ti45Al2Mn2Nb-0.8vol.% TiB2 alloy," *Intermetallics*, vol. 54, pp. 49–55, 2014.
[96] Z. W. Huang and S. Huang, "On the role of thermal exposure on the stress controlled fatigue behaviour of an intermediate strength γ-tial based alloy," *Materials Science and Engineering: A*, vol. 636, pp. 77–90, 2015.
[97] H. Inui, M. H. Oh, A. Nakamura, and M. Yamaguchi, "Room-temperature tensile deformation of polysynthetically twinned (PST) crystals of TiAl," *Acta Metallurgica et Materialia*, vol. 40, no. 11, pp. 3095–3104, 1992.
[98] H. Y. Kim and K. Maruyama, "Parallel twinning during creep deformation in soft orientation PST crystal of TiAl alloy," *Acta Materialia*, vol. 49, no. 14, pp. 2635–2643, 2001.
[99] W. J. Porter, M. D. Uchic, R. John, and N. B. Barnas, "Compression property determination of a gamma titanium aluminide alloy using micro-specimens," *Scripta Materialia*, vol. 61, no. 7, pp. 678–681, 2009.
[100] M. Rester, F. D. Fischer, C. Kirchlechner, T. Schmoelzer, H. Clemens, and G. Dehm, "Deformation mechanisms in micron-sized PST TiAl compression samples: Experiment and model," *Acta Materialia*, vol. 59, no. 9, pp. 3410–3421, 2011.
[101] A. J. Palomares-Garca, M. T. Prez-Prado, and J. M. Molina-Aldareguia, "Effect of lamellar orientation on the strength and operating deformation mechanisms of fully lamellar TiAl alloys determined by micropillar compression," *Acta Materialia*, vol. 123, pp. 102–114, 2017.
[102] T. E. J. Edwards, F. Di Gioacchino, R. Muñoz-Moreno, and W. J. Clegg, "Deformation of lamellar TiAl alloys by longitudinal twinning," *Scripta Materialia*, vol. 118, pp. 46–50, 2016.
[103] T. E. J. Edwards, F. Di Gioacchino, G. Mohanty, J. Wehrs, J. Michler, and W. J. Clegg, "Longitudinal twinning in a TiAl alloy at high temperature by in situ microcompression," *Acta Materialia*, vol. 148, pp. 202–215, 2017.
[104] S. Liu, J. M. Wheeler, P. R. Howie, X. T. Zeng, J. Michler, and W. J. Clegg, "Measuring the fracture resistance of hard coatings," *Applied Physics Letters*, vol. 102, no. 17, p. 171907, 2013.
[105] F. Appel, U. Christoph, and R. Wagner, "An electron microscope study of deformation and crack propagation in (α2 + γ) titanium aluminides," *Philosophical Magazine A*, vol. 72, no. 2, pp. 341–360, 1995.
[106] M. Yamaguchi, D. R. Johnson, H. N. Lee, and H. Inui, "Directional solidification of TiAl-base alloys," *Intermetallics*, vol. 8, no. 5, pp. 511–517, 2000.

[107] X. Li, J. Fan, Y. Su, D. Liu, J. Guo, and H. Fu, "Lamellar orientation and growth direction of α phase in directionally solidified Ti-46Al-0.5W-0.5Si alloy," *Intermetallics*, vol. 27, pp. 38–45, 2012.

[108] X. F. Ding, J. P. Lin, L. Q. Zhang, Y. Q. Su, and G. L. Chen, "Microstructural control of tialnb alloys by directional solidification," *Acta Materialia*, vol. 60, no. 2, pp. 498–506, 2012.

[109] L. Zhang, J. Lin, J. He, J. Yin, and X. Ding, "Influence of thermal stabilization treatment on the subsequent microstructure development during directional solidification of a Ti46Al5Nb alloy," *Intermetallics*, vol. 63, pp. 67–72, 2015.

[110] T. Liu, L. Luo, Y. Su, J. Guo, and H. Fu, "Lamellar orientation control of Ti47Al0.5W0.5Si by directional solidification using β seeding technique," *Intermetallics*, vol. 73, pp. 1–4, 2016.

[111] W. Wan, B. Han, W. Han, and J. Zhang, "High-cycle fatigue behavior of TiAl alloy containing preferentially oriented lamellar microstructures," *Journal of Aeronautical Materials*, vol. 36, no. 1, pp. 87–92, 2016.

[112] H. Shiota, K. Tokaji, and Y. Ohta, "Influence of lamellar orientation on fatigue crack propagation behavior in titanium aluminide TiAl," *Materials Science and Engineering: A*, vol. 243, no. 1, pp. 169–175, 1998.

[113] M. Schütze, "Recent advances in the understanding of the halogen effect in the oxidation of intermetallic titanium aluminides," in *Proceedings - Electrochemical Society*, vol. PV 2004-16, pp. 1–15, 2004.

[114] F. A. Schweizer and D. N. Duhl, "Single crystal nickel superalloy," 1980. Patent.

[115] H. Clemens, H. Kestler, N. Eberhardt, and W. Knabl in *Gamma Titanium Aluminides 1999* (Y.-W. Kim, D. M. Dimiduk, and M. H. Loretto, eds.), p. 209, TMS, 1999.

[116] D. Hu, "Role of boron in TiAl alloy development: a review," *Rare Metals*, vol. 35, no. 1, pp. 1–14, 2015.

[117] J. Yang, H. Li, D. Hu, N. Martin, and M. Dixon, "Lamellar orientation effect on fatigue crack propagation threshold in coarse grained Ti46Al8Nb," *Materials Science and Technology*, vol. 30, no. 15, pp. 1905–1910, 2014.

[118] T. Fujiwara, A. Nakamura, M. Hosomi, S. R. Nishitani, Y. Shirai, and M. Yamaguchi, "Deformation of polysynthetically twinned crystals of TiAl with a nearly stoichiometric composition," *Philosophical Magazine A*, vol. 61, no. 4, pp. 591–606, 1990.

[119] M. Nomura, M.-C. Kim, V. Vitek, and D. Pope in *Gamma Titanium Aluminides 1999* (Y.-W. Kim, D. M. Dimiduk, and M. H. Lorenz, eds.), p. 67, TMS, 1999.

[120] S. Beretta, M. Filippini, P. L., G. Pasquero, and S. Sabbadini, "Fatigue properties and design criteria of a gamma titanium aluminide alloy," *Key Engineering Materials*, vol. 465, pp. 531–534, 2011.

[121] D. Hu, A. Huang, H. Jiang, N. Mota-Solis, and X. Wu, "Pre-yielding and pre-yield cracking in TiAl-based alloys," *Intermetallics*, vol. 14, no. 1, pp. 82–90, 2006.

[122] R. Muñoz-Moreno, M. T. Pérez-Prado, J. Llorca, E. M. Ruiz-Navas, and C. J. Boehlert, "Effect of stress level on the high temperature deformation and fracture mechanisms of Ti-45Al-2Nb-2Mn-0.8 vol. pct TiB2: An in situ experimental study," *Metallurgical and Materials Transactions A*, vol. 44, no. 4, pp. 1887–1896, 2013.

[123] T. E. J. Edwards, F. Di Gioacchino, and W. J. Clegg, "An experimental study of polycrystalline plasticity in lamellar titanium aluminide," unpublished data.

[124] Y. N. Lenets and T. Nicholas, "Load history dependence of fatigue crack growth thresholds for a Ti-alloy," *Engineering Fracture Mechanics*, vol. 60, no. 2, pp. 187–203, 1998.

[125] T. Nicholas, *High cycle fatigue: a mechanics of materials perspective*. Elsevier, 2006.

[126] R. Pippan, P. Hageneder, W. Knabl, H. Clemens, T. Hebesberger, and B. Tabernig, "Fatigue threshold and crack propagation in γ-TiAl sheets," *Intermetallics*, vol. 9, no. 1, pp. 89–96, 2001.

[127] B. A. Lerch, S. L. Draper, and J. M. Pereira, "Conducting high-cycle fatigue strength step tests on gamma TiAl," *Metallurgical and Materials Transactions*, vol. 33A, no. 12, pp. 3871–3874, 2002.

[128] A. J. Wilkinson, G. Meaden, and D. J. Dingley, "High resolution mapping of strains and rotations using electron backscatter diffraction," *Materials Science and Technology*, vol. 22, no. 11, pp. 1271–1278, 2006.

[129] P. Beran, M. Heczko, T. Kruml, T. Panzner, and S. van Petegem, "Complex investigation of deformation twinning in γ-TiAl by TEM and neutron diffraction," *Journal of the Mechanics and Physics of Solids*, vol. 95, pp. 647–662, 2016.

[130] M. A. Sutton, J. J. Orteu, and H. Schreier, *Image correlation for shape, motion and deformation measurements: basic concepts, theory and applications*. Springer Science & Business Media, 2009.

[131] A. Orozco-Caballero, D. Lunt, J. D. Robson, and J. Quinta da Fonseca, "How magnesium accommodates local deformation incompatibility: A high-resolution digital image correlation study," *Acta Materialia*, vol. 133, pp. 367–379, 2017.

[132] H. Jiang, F. A. Garcia-Pastor, D. Hu, X. Wu, M. H. Loretto, M. Preuss, and P. J. Withers, "Characterization of microplasticity in TiAl-based alloys," *Acta Materialia*, vol. 57, no. 5, pp. 1357–1366, 2009.

[133] T. Niendorf, C. Burs, D. Canadinc, and H. J. Maier, "Early detection of crack initiation sites in TiAl alloys during low-cycle fatigue at high temperatures utilizing digital image correlation," *International journal of materials research*, vol. 100, no. 4, pp. 603–608, 2009.

[134] L. Patriarca, M. Filippini, and S. Beretta, "Digital image correlation-based analysis of strain accumulation on a duplex γ-TiAl," *Intermetallics*, vol. 75, pp. 42–50, 2016.

[135] L. Patriarca, C. Içöz, M. Filippini, and S. Beretta, "Microscopic analysis of fatigue damage accumulation in TiAl intermetallics," *ASME Turbo Expo 2014: Turbine Technical Conference and Exposition*, vol. 7A, 2014.

[136] C. Içöz, L. Patriarca, M. Filippini, and S. Beretta, "Strain accumulation in TiAl intermetallics via high-resolution digital image correlation (DIC)," *Procedia Engineering*, vol. 74, no. 0, pp. 443–448, 2014.

[137] F. Di Gioacchino and J. Quinta da Fonseca, "Plastic strain mapping with sub-micron resolution using digital image correlation," *Experimental Mechanics*, vol. 53, no. 5, pp. 743–754, 2012.

[138] T. E. J. Edwards, F. Di Gioacchino, H. P. Springbett, R. A. Oliver, and W. J. Clegg, "Stable speckle patterns for nano-scale strain mapping up to 700C," *Experimental Mechanics*, 2017.

[139] M. A. Sutton, N. Li, D. C. Joy, A. P. Reynolds, and X. Li, "Scanning electron microscopy for quantitative small and large deformation measurements part I: Sem imaging at magnifications from 200 to 10,000," *Experimental Mechanics*, vol. 47, no. 6, pp. 775–787, 2007.

[140] M. A. Sutton, N. Li, D. Garcia, N. Cornille, J. J. Orteu, S. R. McNeill, H. W. Schreier, X. Li, and A. P. Reynolds, "Scanning electron microscopy for quantitative small and large deformation measurements part II: experimental validation for magnifications from 200 to 10,000," *Experimental Mechanics*, vol. 47, no. 6, pp. 789–804, 2007.

[141] J. C. Stinville, M. P. Echlin, P. G. Callahan, V. M. Miller, D. Texier, F. Bridier, P. Bocher, and T. M. Pollock, "Measurement of strain localization resulting from monotonic and cyclic loading at 650 C in nickel base superalloys," *Experimental Mechanics*, vol. 57, no. 8, p. 12891309, 2017.

[142] T. Pfullmann and P. A. Beaven, "On the relationship between lattice parameters and composition of the γ-TiAl phase," *Scripta Metallurgica et Materialia*, vol. 28, no. 3, pp. 275–280, 1993.

[143] X. F. Zhang, Q. Yang, L. C. De Jonghe, and Z. Zhang, "Energy dispersive spectroscopy analysis of aluminium segregation in silicon carbide grain boundaries," *Journal of Microscopy*, vol. 207, no. 1, pp. 58–68, 2002.

[144] A. Huguet and A. Menand, "Atom-probe determination of interstitial element concentration in two-phase and single-phase TiAl-based alloys," *Applied Surface Science*, vol. 76, pp. 191–197, 1994.

[145] A. Menand, H. Zapolsky-Tatarenko, and A. Nrac-Partaix, "Atom-probe investigations of TiAl alloys," *Materials Science and Engineering: A*, vol. 250, no. 1, pp. 55–64, 1998.
[146] T. Klein, F. Mendez-Martin, M. Schachermayer, B. Rashkova, H. Clemens, and S. Mayer, "Distribution of alloying elements within the constituent phases of a C-containing γ-TiAl based alloy studied by atom probe tomography," *MRS Proceedings*, vol. 1760, 2015.
[147] W. Lefebvre, A. Loiseau, and A. Menand, "Field evaporation behaviour in the γ phase in TiAl during analysis in the tomographic atom probe," *Ultramicroscopy*, vol. 92, no. 2, pp. 77–87, 2002.
[148] T. Klein, H. Clemens, and S. Mayer, "Advancement of compositional and microstructural design of intermetallic γ-TiAl based alloys determined by atom probe tomography," *Materials*, vol. 9, no. 9, p. 755, 2016.
[149] T. Klein, L. Usategui, B. Rashkova, M. L. N, J. San Juan, H. Clemens, and S. Mayer, "Mechanical behavior and related microstructural aspects of a nano-lamellar TiAl alloy at elevated temperatures," *Acta Materialia*, vol. 128, pp. 440–450, 2017.
[150] G. Sernicola, T. Giovannini, P. Patel, J. R. Kermode, D. S. Balint, T. B. Britton, and F. Giuliani, "In situ stable crack growth at the micron scale," *Nature Communications*, vol. 8, no. 1, p. 108, 2017.
[151] Y. Xiao, J. Wehrs, H. Ma, T. Al-Samman, S. Korte-Kerzel, M. Göken, J. Michler, R. Spolenak, and J. M. Wheeler, "Investigation of the deformation behavior of aluminum micropillars produced by focused ion beam machining using Ga and Xe ions," *Scripta Materialia*, vol. 127, pp. 191–194, 2017.
[152] M. H. Yoo and C. L. Fu, "Physical constants, deformation twinning, and microcracking of titanium aluminides," *Metallurgical and Materials Transactions A*, vol. 29, no. 1, pp. 49–63, 1998.